Volume 7 | Number 18 | 21 September 2020

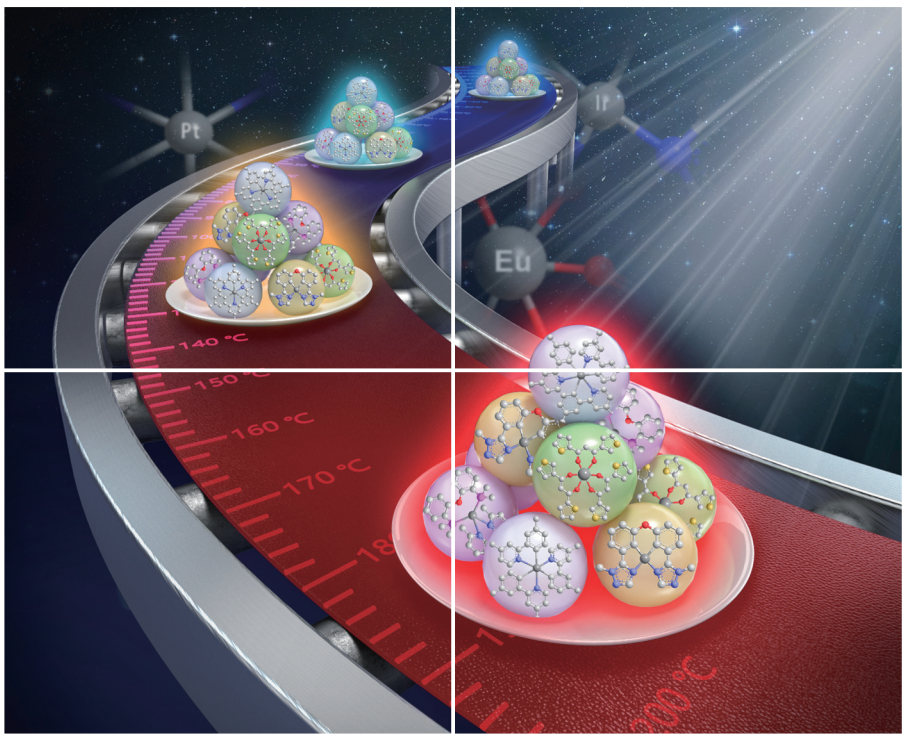

INORGANIC CHEMISTRY

FRONTIERS

CCS 中国化学会 CHINESE CHEMICAL SOCIETY
PEKING UNIVERSITY 1898
ROYAL SOCIETY OF CHEMISTRY
rsc.li/frontiers-inorganic

INORGANIC CHEMISTRY
FRONTIERS

REVIEW

View Article Online
View Journal | View Issue

Cite this: *Inorg. Chem. Front.*, 2020, **7**, 3258

Thermo-responsive light-emitting metal complexes and related materials

Rui Li, †[a,b] Fa-Feng Xu, †[a] Zhong-Liang Gong *[a] and Yu-Wu Zhong *[a,b]

Thermo-responsive light-emitting materials have wide potential applications in temperature sensing, bio-imaging, optoelectronic devices and information security, due to their intriguing luminescence property changes in response to temperature. Among them, light-emitting metal complexes and related coordination materials are appealing in possessing enormous structural diversity and excellent luminescence properties. The general thermo-responsive types and the underlying mechanism of these materials and recent progress in the development of thermo-responsive metal complexes and related materials are surveyed in this critical review, including small molecular metal complexes with different electronic configurations (d^6, d^8, d^{10}, among others), metal clusters, coordination polymers, metal–organic frameworks (MOFs), and multicomponent coordination polymers and assemblies. A particular focus is given on how to build systems showing ratiometric lumunescence changes in response to temperature, including molecular dyads containing two chromophores, heterodimetallic clusters, mixed-metal MOFs, and energy donor–acceptor assemblies. In addition, the applications of these materials in temperature sensing, bio-imaging, and information security are briefly discussed. A perspective is given in the Conclusion section to reflect potential guidelines for future research in this field.

Received 2nd July 2020,
Accepted 26th July 2020

DOI: 10.1039/d0qi00779j

rsc.li/frontiers-inorganic

1. Introduction

Temperature is one of the most fundamental physical parameters in scientific research and industrial production. The variation of temperature may lead to distinct changes of the chemical and physical properties of natural systems and synthetic materials.[1–4] In particular, thermo-responsive functional materials with specific luminescence changes have attracted wide attention due to their potential applications in temperature sensing,[5–12] biological imaging,[13–20] optoelectronic devices,[21–25] and information processing.[26–28] To date, tremendous progress has been made in

[a]*Beijing National Laboratory for Molecular Sciences, CAS Key Laboratory of Photochemistry, CAS Research/Education Center for Excellence in Molecular Sciences, Institute of Chemistry, Chinese Academy of Sciences, Beijing 100190, China. E-mail: gongzhongliang@iccas.ac.cn, zhongyuwu@iccas.ac.cn*
[b]*School of Chemical Sciences, University of Chinese Academy of Sciences, Beijing 100049, China*
† These authors contributed equally to this work.

Rui Li

Rui Li received her B.S. degree from Central China Normal University in 2015. She is currently a Ph.D. candidate at the Institute of Chemistry, Chinese Academy of Sciences, under the supervision of Prof. Yu-Wu Zhong. Her research interests focus on emissive metal complexes and their assembled structures.

Fa-Feng Xu

Fa-Feng Xu obtained his B.S. degree from Jilin University in 2014 and Ph.D. from the Institute of Chemistry, Chinese Academy of Sciences (ICCAS) in 2020 under the supervision of Prof. Jiannian Yao and Prof. Yong Sheng Zhao. Currently, he works as a postdoctoral fellow with Prof. Yu-Wu Zhong at ICCAS. His research interests focus on the fabrication and application of organic luminescent materials and micro/nano lasers.

the development of thermo-responsive light-emitting materials, including various organic dyes and polymers,[29–37] metal complexes,[38–44] metal clusters and metal–organic frameworks (MOFs),[45–49] quantum dots (QDs),[50,51] and nanomaterials.[52–55]

Among the abovementioned materials, metal complexes and related coordination materials have several outstanding advantages.[56–59] Metal complexes are known to possess various metal–ligand coordination modes, such as linear, planar, tetrahedral, and octahedral configurations. They are characterized by rich radiative excited states, including the intra-ligand (IL) or ligand-centered (LC) transition, the metal-to-ligand or ligand-to-metal charge-transfer (MLCT or LMCT) transition, the ligand-to-ligand charge-transfer (LLCT) transition, the metal–metal-to-ligand charge-transfer (MMLCT) transition, and the cluster/metal-centered (MC) transition. Due to the strong spin–orbit coupling effect, metal complexes often display triplet luminescence, namely phosphorescence, with long excited-state lifetimes (τ) and good to excellent quantum yields (ϕ). However, the involvement of ligand-related singlet fluorescence is also possible, leading to the co-presence or overlap of multiple radiative transitions. These features allow us to modulate the chemical compositions and luminescence properties of metal complexes in a wide emission spectral coverage from the ultraviolet (UV) to near-infrared (NIR) region that could respond to temperature changes in a wide temperature range.

Several reviews focusing on thermo-responsive MOFs and lanthanide or Cu-based clusters have been published recently;[2–4,60] however temperature-responsive metal complexes in a broader scope have not been reviewed. We present here a systematic summary and discussion on thermo-responsive metal complexes including small molecular metal complexes, metal–ligand coordination clusters and polymers, and related multi-component materials. Considering that a great number of related complexes and materials have been reported in this field, only some representative and latest examples are in particular selected for discussions. In this sense, the article is structured mainly in four aspects: (1) the outline of general thermo-responsive types and underlying mechanism; (2) thermo-responsive small molecular metal complexes, including those with d^6, d^8, d^{10} and other electronic configurations and lanthanide complexes; (3) thermo-responsive metal clusters, coordination polymers (CPs), and MOFs; (4) multi-component CPs and assemblies. These discussions are followed by some guided perspectives for future research in the Conclusion section.

2. General thermo-responsive types and underlying mechanism

The thermal responsiveness of materials could be caused by a number of different factors. Firstly, the non-radiative rate constant k_{nr} increases with increasing temperatures, obeying the Arrhenius equation (2.1),

$$k_{nr} \sim e^{(-\Delta E/kT)} \quad (2.1)$$

where ΔE represents the energy gap between the level of the lowest excited state and the overlap point to non-radiative transition states, and k is the Boltzmann constant.[1,3] For a simple molecular system, the emission intensity (I) is dependent on temperature, considering that I is proportional to ϕ and ϕ is in inverse proportion to k_{nr} according to eqn (2.2),

$$\phi = k_r/(k_r + k_{nr}) \quad (2.2)$$

where k_r is the radiative rate constant. In this sense, all emissive materials are intrinsically thermo-responsive.

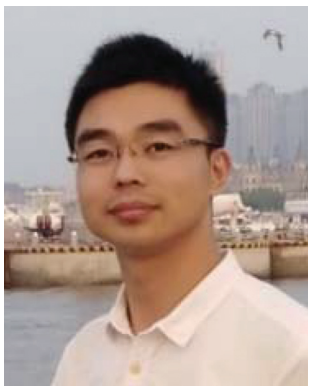

Zhong-Liang Gong

Zhong-Liang Gong received his Ph.D. degree from the Institute of Chemistry, Chinese Academy of Sciences under the supervision of Prof. Yu-Wu Zhong in 2015. After that, he worked as an assistant professor in the same research group and was promoted as an associate professor in 2020. His current interests mainly focus on the synthesis and optoelectronic applications of luminescent transition metal complexes.

Yu-Wu Zhong

Yu-Wu Zhong obtained his Ph.D. in 2004 from the Shanghai Institute of Organic Chemistry, Chinese Academy of Sciences. After that, he worked as a post-doctoral associate at the University of Tokyo (2004–2006) and Cornell University (2006–2009), respectively. He joined the Institute of Chemistry, Chinese Academy of Sciences, to start his independent career in 2009. He received the China Electrochemistry Young Scientist Award in 2015, the China Photochemistry Young Scientist Award, the National Science Fund for Distinguished Young Scholars, and the Chinese Chemical Society-Evonik Chemical Innovation Award for Distinguished Scientist in 2019. His current research interests focus on the synthesis, assembly, and applications of photo- and electro-functional molecular materials.

In addition to the thermal-activated non-radiative decay, many other factors may be activated or influenced by temperature, including the effective molecular conformation or configuration transformation of flexible systems,[61,62] the degree of inter- or intramolecular π–π stacking and metal–metal interactions existing in aggregates or clusters of Rh(I), Pt(II), Cu(I), Ag(I), and Au(I) complexes,[39,63–65] the dynamic association or dissociation process of metal and lanthanide complexes,[66,67] phase transition,[68–71] the degree of inter- or intramolecular energy transfer of donor/acceptor systems,[72,73] as well as the thermal equilibrium of different excited states.[74,75] These mechanisms will be discussed in more detail in specific examples in the following chapters.

In general, four types of readouts are employed to characterize the thermo-responsiveness of materials, including the change of emission intensity, maximum emission wavelength (λ_{emi}), emission lifetime, and emission polarization (or anisotropy).[1,3] The sensitivity of a particular process is defined as the slope of the readout signal change as a function of temperature, usually expressed as percent change per Kelvin (% K^{-1}), which is an important indicator for evaluating temperature-sensitive materials. The intensity-based thermo-responsiveness is the simplest process. As was discussed above, the thermal-activated non-radiative decay could lead to the variation of emission intensity. However, the emission intensity changes could also be caused by many other factors, such as the dynamic association/dissociation process or phase transition.[66,71] The shift of λ_{emi} is another general readout during the studies of thermo-responsive materials, which could be a result of dynamic thermal-equilibrium of different excited states or the change of the energy/electron transfer efficiency.[76,77] The shift of λ_{emi} often leads to the emission color changes of materials, allowing us to conveniently monitor the thermo-responsive process. Compared to the emission intensity, the emission lifetime is less dependent on conditions such as photo-bleaching, concentration of materials, and energy fluctuation of the excitation source. It presents another important readout to monitor the thermo-responsiveness. Lifetime-based thermo-responsible materials have potential applications in time-resolved biological imaging and cellular temperature monitoring.[78,79] The last readout is emission polarization or anisotropy, which generally decreases with increasing temperature as a result of the temperature-dependent Brownian motion of individual molecules.[80] For more detailed discussions on the thermo-responsive mechanism and readouts, the authors are directed to a previous review article.[1]

3. Thermo-responsive small molecular metal complexes

Small molecular discrete metal complexes possess good thermo and photostability and rich luminescence in a broad spectral range. Their thermo-responsive behaviour accompanied by luminescence property changes has received much interest. In this section, some representative examples with different electronic configurations (d^6, d^8, d^{10}, and others and lanthanide complexes) are discussed.

3.1 d^6 metal complexes

Luminescent metal complexes with a d^6 electronic configuration mainly include Re(I), Ru(II), Os(II), Rh(III), and Ir(III) complexes, which exhibit remarkable luminescence properties and are extensively used in OLEDs and chemical sensing.[81–84] The applications of emissive Ru(II) complexes in temperature sensing are well established.[85,86] For instance, Orellana and coworkers show that the luminescence lifetimes of a series of Ru(II) polyazaheteroaromatic complexes **1a–1f** decrease in accordance with the Arrhenius equation (Fig. 1).[85] These complexes are further embedded into poly(ethyl cyanoacrylate) as the responsive media to sense temperature. By taking fully advantage of the low permeability to O_2, excellent optical quality, and high temperature-sensitive luminescence intensity and lifetimes, the doped film of **1c** demonstrated a sensing resolution of 0.05 °C with a linear response to temperature in the range of 0–40 °C based on the lifetime readout. These features make it potentially applicable for temperature monitoring in bioreactor and biological tissues.

Ir(III) complexes are another important thermochromic luminescent d^6 metal complexes.[87–89] For example, Zhao, Huang and coworkers have reported a series of thermo-responsive Ru(II) and Ir(III) complexes functionalized with methyl pyridinium chromophores.[89] Shown in Fig. 2 are the results of a representative Ir(III) complex **2**. This complex is only weakly

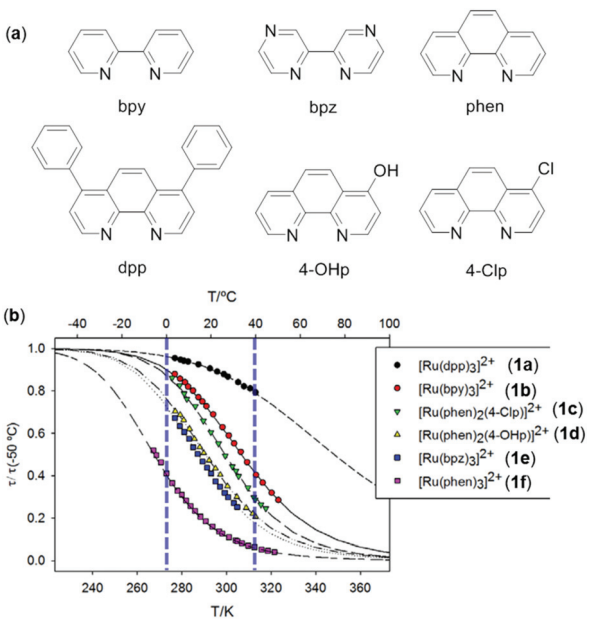

Fig. 1 (a) Bidentate ligands to make ruthenium complexes **1a–1f**. (b) Luminescence lifetimes (normalized at 50 °C) as a function of temperature of **1a–1f** (counter anions are Cl^-) in deoxygenated propylene carbonate solution. Reprinted with permission from ref. 85. License MDPI, Basel, Switzerland.

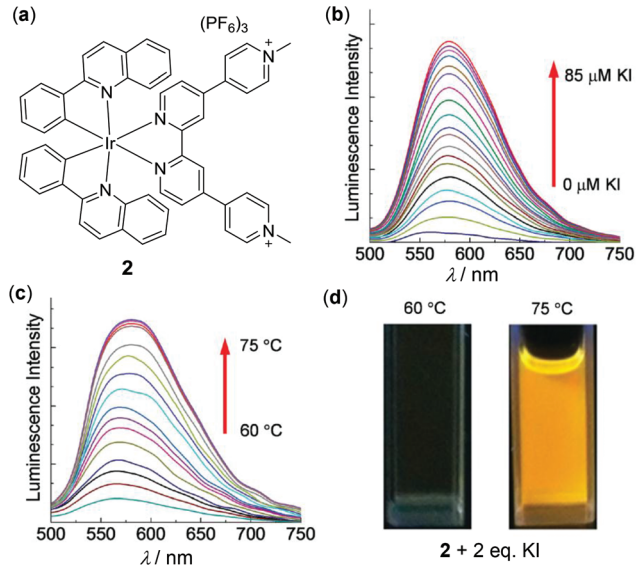

Fig. 2 (a) Molecular structure of Ir(III) complex **2**. (b) Luminescence spectra change of **2** in degassed CH_3CN (1.0×10^{-5} M) at 75 °C with an increasing amount of KI from 0 to 10 equiv. (c) Temperature-dependent luminescence spectral change of **2** with 2 equiv. of KI upon heating from 60 to 75 °C. (d) Photographs of the solution of **2** at 60 or 75 °C in the presence of 2 equiv. of KI. Reprinted with permission from ref. 89. Copyright 2016 WILEY-VCH.

emissive (Φ < 0.1%) in degassed CH_3CN, caused by oxidative quenching of the deficient methyl pyridinium unit *via* intramolecular electron transfer. However, when the methyl pyridinium units are reduced, the luminescence of **2** can be strongly enhanced *in situ*. In particular, the reduction of **2** by KI is remarkably temperature-dependent. At 60 °C or below, no reduction occurs. When the temperature is increased from 60 to 75 °C, the reduction occurs smoothly accompanied by a significant yellow-emission enhancement. On the basis of the synergy between KI and temperature, a novel information protection device has been fabricated with complex **2**.

The above example demonstrates the thermo-responsive behaviour by controlling the electron transfer process. It is also possible to utilize the intramolecular energy transfer process to realize thermo-responsive properties. For instance, the Ir(III)-naphthalimide dyad **3** displays dual emissions at 507 and 606 nm at 77 K in cryogenic Me-THF, originating from the ^{3}LC emission of the naphthalimide unit and the ^{3}MLLCT (metal/ligand-to-ligand charge-transfer) emission of the Ir(III) component, respectively.[90] In contrast, complex **3** only shows a single broad and unstructured ^{3}MLLCT emission at 593 nm (τ = 8.8 ms) at rt due to the efficient energy transfer process from the naphthalimide unit to the Ir(III) component.

3.2 d^8 metal complexes

Metal complexes with a d^8 electronic configuration, *e.g.* Rh(I), Pd(II) and Pt(II) complexes, are another type of important luminescent material.[56] In particular, widespread attention has been paid to square planar Pt(II) complexes as thermo-responsive materials in recent years.[91–98] These complexes are prone to form intermolecular metal–metal or π–π interactions in aggregate states, which is highly dependent on external conditions such as concentration and temperature. For instance, Wang and coworkers reported the tetradentate Pt(II) complex **4**, which displayed distinguished temperature-responsive luminescence (Fig. 4a and b).[91] Only one structured monomeric blue emission at 477 nm was observed for complex **4** in degassed Me-THF (1×10^{-3} M) at temperatures below 130 K. However, as the temperature increased from 130 to 345 K, a new unstructured excimer emission at 650 nm appeared, accompanied by a dramatic emission color change from sky-blue to red. This luminescent thermochromism is fully reversible and reproducible. The authors deduced that the red emission was due to π-stacked excimers as elevated temperatures tended to increase the kinetic energy of the molecules and the probability of forming excimers. Similarly, the formation of the ^{3}MMLCT transition *via* inter- or intramolecular Pt–Pt interactions is also strongly dependent on temperature. In this

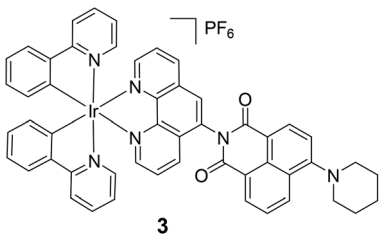

Fig. 3 Thermo-responsive Ir(III) complex **3** on the basis of the controlled energy transfer mechanism. Reprinted with permission from ref. 90. Copyright 2016 Wiley-VCH.

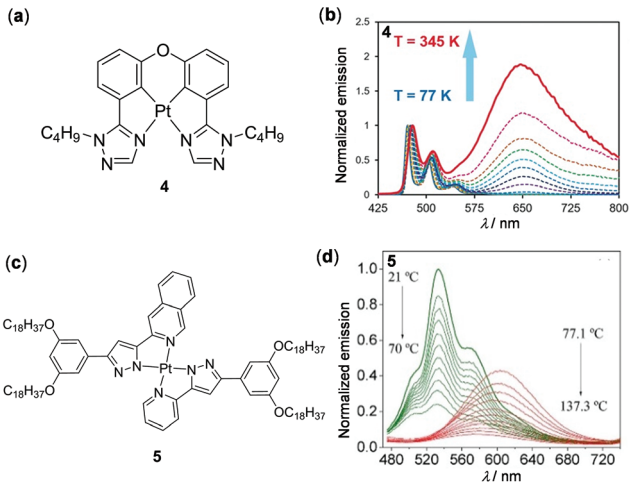

Fig. 4 (a) Molecular structure of Pt(II) complex **4**. (b) Normalized temperature-dependent emission spectra of **4** in degassed Me-THF (1×10^{-3} M, λ_{ex} = 397 nm). Reprinted with permission from ref. 91. Copyright 2017 Wiley-VCH. (c) Molecular structure of Pt(II) complex **5**. (d) Normalized temperature-dependent emission spectral changes of the PMMA film doped with **5** upon heating from 21 to 137.3 °C. Reprinted with permission from ref. 92. Copyright 2020 Elsevier Ltd.

context, Lodeiro and coworkers prepared luminescent polymers by doping the bis(pyrazolate) Pt(II) complex **5** into PMMA, which showed interesting multistep thermochromic luminescence (Fig. 4c and d).[92] With an increase of temperature from 21 to 137.3 °C, three-step emission changes were clearly observed. Within the temperature range between 21 and 70 °C, the original greenish emission gradually decreased due to the aggregation-caused quenching (ACQ) effect. An orange emission in the lower-energy region appeared at 70–75 °C, attributed to the formation of the ^{3}MMLCT excited state *via* intermolecular Pt–Pt interactions. When the temperature was further increased from 77 to 137 °C, the ^{3}MMLCT emission was progressively quenched, caused by the thermally-activated non-radiative transition process. This Pt(II) complex provides a potential candidate for the preparation of multistep thermochromic materials.

The above two examples demonstrate the thermoresponsive behaviour of Pt complexes as a result of the changes of intermolecular interactions. As an example of thermo-responsive Pt(II) complexes by manipulating the intramolecular Pt–Pt interactions, Yam and coworkers showed that a series of oligo(ethynylpyridine)-bridged diplatinum metallofoldamers, represented by complex **6** in Fig. 5, displayed reversible emission color changes between green and red as a result of the solvent or temperature-controlled helix–coil configuration transformation.[93]

As has been discussed above in the case of Ir(III)-naphthalimide complex **3** (Fig. 3), thermal-equilibrium of different excited states in molecules containing two or more than two chromophores is an effective strategy to induce thermo-responsive properties. Using a similar strategy, Zhao and coworkers prepared the platinum bis(acetylide) complex **7** with the incorporations of two naphthalimide units on the acetylide ligand (Fig. 6).[96] Two closely-lying triplet excited states, *i.e.* ^{3}MLCT and the naphthalimide-localized emissive triplet state (^{3}LE), co-exist in this complex, the population ratio of which could be finely tuned by solvent polarity and temperature. For instance, upon heating from 298 to 358 K, the ^{3}LE emission of **7** at 605 nm diminished whereas the ^{3}MLCT emission at 565 nm was intensified in toluene. However, when measured

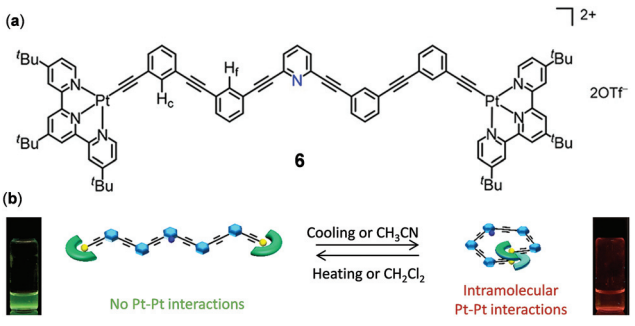

Fig. 5 (a) Molecular structure of Pt(II) complex **6**. (b) Schematic diagram showing the reversible helix–coil molecular configuration transformation regulated by solvents and temperature. Reprinted with permission from ref. 93. Copyright 2019 American Chemical Society.

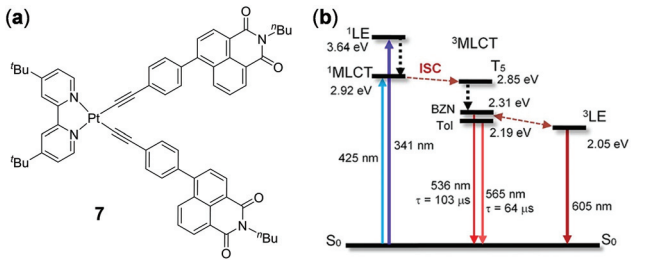

Fig. 6 (a) Molecular structure of Pt(II) complex **7**. (b) Simplified Jablonski diagram showing the energy levels of **7**. BZN = benzonitrile. Tol = toluene. Reprinted with permission from ref. 96. Copyright 2019 American Chemical Society.

in benzonitrile, the ^{3}MLCT emission of **7** at 536 nm was only slightly increased upon heating to 363 K; however the ^{3}LE emission at 620 nm was dramatically decreased. This work demonstrates the importance of thermo-responsive behaviour in understanding the intrinsic photophysical properties of light-emitting materials containing multiple chromophores.

As an example of thermo-responsive Pt(II) complexes with more complex molecular structures, Zhong, Stang, and coworkers examined two fluorescent hexagonal organoplatinum metallacycles **8a** and **8b** with appended anthracene chromophores (Fig. 7).[97] Upon increasing the temperature from −20 to 60 °C, the emission of **8a** and **8b** at 520 nm in THF was gradually decreased with a sensitivity of −0.66% and −0.76% per °C, ascribed to the accelerated molecular rotation of the appended anthracene units. In addition, complex **8a** displayed two-step temperature-dependent emission spectral changes in DMF. Upon heating from −20 to 30 °C, the emission at 530 nm was gradually decreased. Upon further heating from 30 to 70 °C, this emission band shifted to 470 nm with a diminished intensity. Concurrently, a distinct emission color change from green to cyan was clearly visualized. However, the emission shift in the second step is irreversible, which is caused by the decomposition of the metallacycle by DMF.

We discussed in this section mainly on the thermo-responsive small molecular complexes. However, it should be pointed out that it is also possible to achieve thermo-responsiveness by incorporating metal complexes into thermosensitive polymeric materials. As an example in this context, Huang, Sun, and coworkers prepared a luminescent polymer **9** by introducing an AIE-active (AIE = aggregation induced emission) Pt(II) component into the thermosensitive poly *N*-isopropylacrylamide backbone through copolymerization (Fig. 8).[98] Upon increasing the temperature from 28 to 39 °C in the physiological range, the yellow emission of **9** in PBS buffer (pH = 7.4) exhibited a significant enhancement due to the rigidified microenvironment of the Pt component induced by the aggregation of polymer chains at elevated temperatures. This thermo-sensitive luminescent polymer material was subsequently applied in intracellular imaging for monitoring the temperature distribution, taking advantage of its high stability and biocompatibility, and the good reversibility of the thermochromic process.

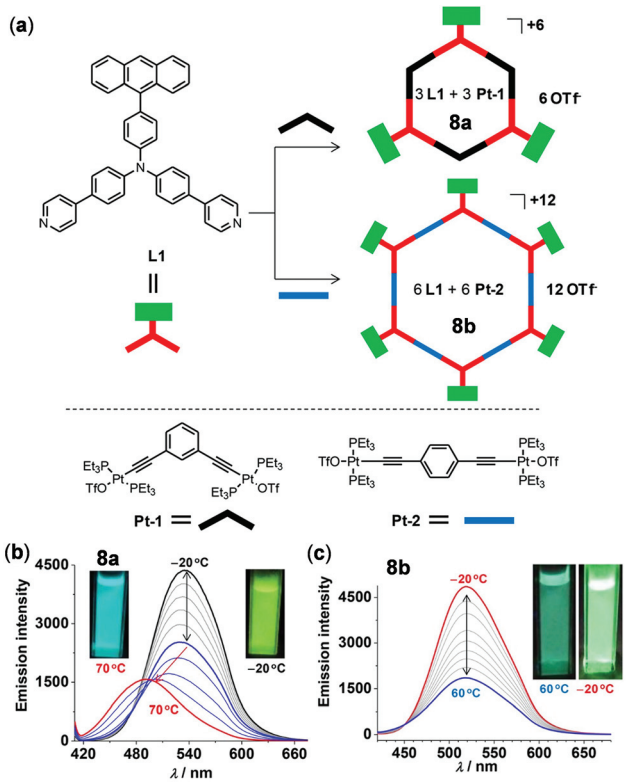

Fig. 7 (a) Synthetic routes and schematic diagram of metallacycles **8a** and **8b**. (b and c) Temperature-dependent emission spectral changes of (b) **8a** in DMF and (c) **8b** in THF (λ_{ex} = 400 nm, 2 × 10^{-5} M). The insets show the emission colors at lower and higher temperature, respectively. Reprinted with permission from ref. 97. Copyright 2018 American Chemical Society.

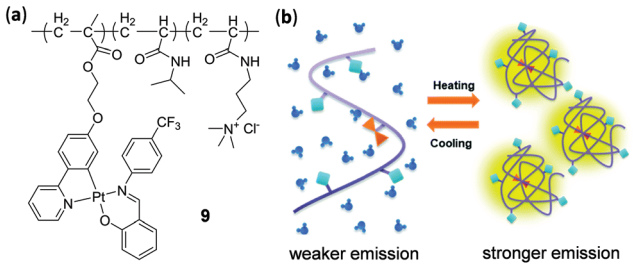

Fig. 8 (a) Polymer **9** with an appended Pt(II) complex. (b) Schematic illustration showing the thermo-responsive mechanism. Reprinted with permission from ref. 98. Copyright 2019 The Royal Society of Chemistry.

3.3 d^{10} metal complexes

In addition to d^6 and d^8 metal complexes, luminescent d^{10} metal complexes, including Cu(I), Ag(I), Au(I), Zn(II), and Cd(II) complexes, have also been demonstrated to display thermo-responsive properties, which will be discussed in this section. As an example of thermo-responsive Cu(I) complexes, Wolf and coworkers reported the thermochromic solid-state emission of the dipyridyl sulfoxide Cu(I) complex **10** (Fig. 9).[99] The crystalline sample (solid or film) of **10** displayed orange emission at

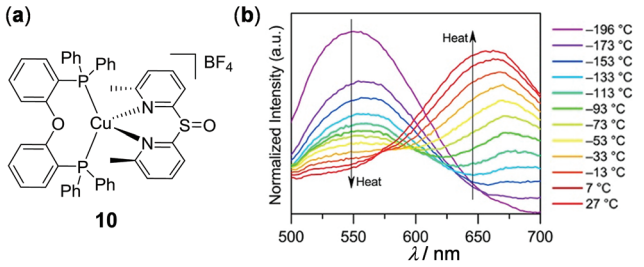

Fig. 9 (a) Molecular structure of Cu(I) complex **10**. (b) Normalized temperature-dependent emission spectral changes of **10** from −196 to 27 °C as thin films by drop-casting on quartz from MeOH solution (λ_{ex} = 380 nm). Reprinted with permission from ref. 99. Copyright 2018 American Chemical Society.

rt. Upon cooling to −190 °C, the orange emission turned to yellow with an emission spectral shift of around 100 nm. The yellow-orange thermochromic luminescence of **10** is fully reversible between −190 and 27 °C, which is ascribed to the excited state coordination geometry change of **10** triggered by temperature (a more flattened state at rt *versus* a pseudo-tetrahedral geometry at −190 °C).

Shown in Fig. 10 is a thermochromic square-planar Ag(I) complex **11** reported by Artem'ev and coworkers. At 298 K, complex **11** exhibited pronounced solid-state yellow emission (λ_{emi} = 585 nm), assigned to the ^{3}MLCT phosphorescence with an admixture of ^{1}MLCT fluorescence. Upon cooling to 77 K, the maximum emission shifted to 620 nm with a concomitant 35% enhancement of intensity and emission color change from yellow to orange-red. This phenomenon was attributed to a small alternation of the ground and excited states of **11**, resulting in a narrowing of the energy gap between the T_1 and S_0 states upon cooling.[77]

In addition to mononuclear metal complexes, d^{10} complexes with multiple metal centers have been reported regarding their thermosensitive properties. Strelnik and coworkers prepared a binuclear Au(I) complex **12** bridged by a flexible bidentate cyclic phosphine ligand (Fig. 11).[100] This complex exhibited very weak greenish emission in solution at rt. Upon cooling to 180 K, a slight blue shift of the emission spectrum with a significant intensity enhancement was observed, mainly

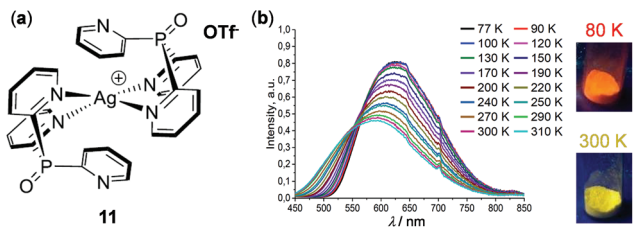

Fig. 10 (a) Molecular structure of Ag(I) complex **11**. (b) Normalized temperature-dependent emission spectral changes in the range of 77–310 K. The pictures on the right show the solid emission colors of the samples at 80 and 300 K, respectively. Reprinted with permission from ref. 77. Copyright 2019 the Partner Organisations.

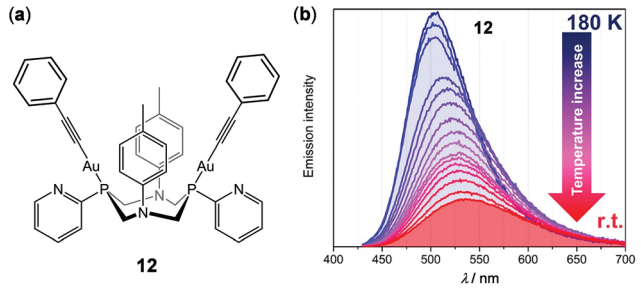

Fig. 11 (a) Molecular structure of Au(I) complex **12**. (b) Temperature-dependent emission spectral changes of **12** in the range of 180–298 K (λ_{ex} = 340 nm). Reprinted with permission from ref. 100. Copyright 2019 American Chemical Society.

attributed to the configuration rigidification of **12** at low temperatures. Upon heating back to 298 K, the initial emission can be completely restored, demonstrating the excellent thermoreversibility of the complex. Besides, a series of cyclic trinuclear Cu(I), Ag(I) and Au(I) complexes **13a–13c** have been prepared by Giménez and coworkers, which exhibited excellent thermochromic luminescence switching (Fig. 12).[101] The gold and copper complexes **13a** and **13c** are highly emissive with Φ > 90% in doped PMMA films (5 wt%) at rt. Upon cooling from 298 to 77 K, the initial red emissions of **13a** and **13c**, originated from centered excimeric (^{3}MM) states *via* intermolecular aurophilic interactions, were gradually transformed into blue and yellow emission, respectively. In contrast, the PMMA film of the silver complex **13b** was not luminescent at rt, but it showed a blue luminescence turn-on upon cooling, demonstrating the important influence of the metal in influencing the photophysical properties.

In addition to the above examples, earth-abundant Zn(II) and Cd(II) complexes are other d^{10} complexes that have been reported to show thermo-responsive luminescence behaviours. For instance, Zhao, Huang, and coworkers have fabricated chameleon-like thermochromic luminescent materials by doping complex Zn-BPPA (**14**) into polyethylene glycol (PEG) matrices (Fig. 13).[102] Complex **14** was prepared from the bipyridine ligand BPPA and it showed completely different emission spectra with respect to BPPA. When 0.3 wt% of **14** was doped into PEG8000, the yellow emission of the obtained material turned blue, accompanied by a distinct intensity enhancement, upon increasing the temperature from 25 to 65 °C. This response is highly reversible (20 cycles of heating and cooling

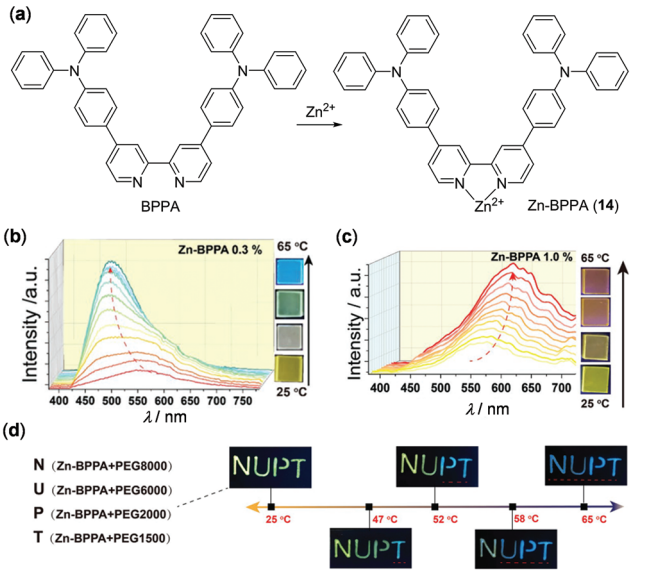

Fig. 13 (a) Chemical structures of BPPA and Zn(II) complex **14**. (b and c) Temperature-dependent emission spectral and color change of PEG8000 containing (b) 0.3 wt% and (c) 1.0 wt% of **14** within the temperature range of 25–65 °C. (d) Photographs displaying thermochromic luminescent NUPT patterns at different temperatures. The letters "N, U, P, and T" were written on a glass substrate using **14**/PEG8000, **14**/PEG6000, **14**/PEG2000 and **14**/PEG1500 composites containing 0.3, 0.3, 0.2, and 0.2 wt% of **14**, respectively. Reprinted with permission from ref. 102. Copyright 2020 WILEY-VCH.

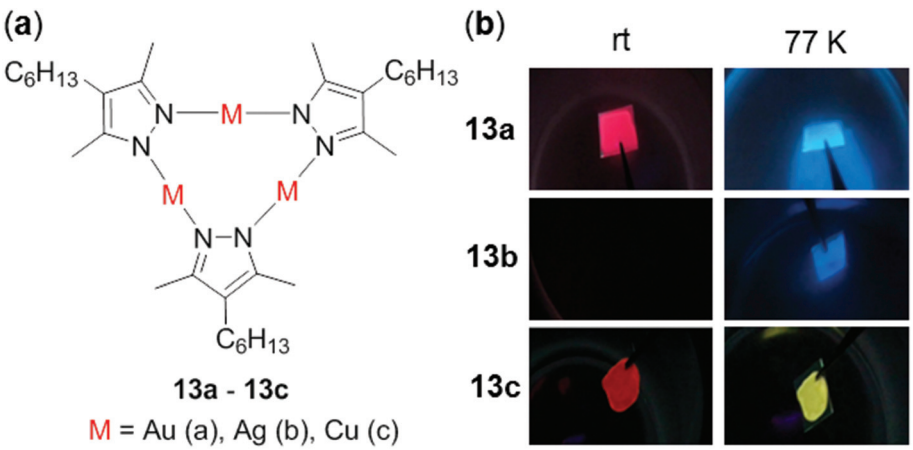

Fig. 12 (a) Molecular structures of complexes **13a–13c**. (b) Video snapshots of the luminescence color switching of PMMA films (5 wt%) excited at 254 nm from rt to 77 K for **13a–13c**. Reprinted with permission from ref. 101. Copyright 2018 American Chemical Society.

being tested) and it functions as a fluorescent thermometer with good sensitivity. The emission spectral changes are caused by the dynamic metal–ligand coordination and dissociation of the BPPA ligand and Zn(II) ions. Interestingly, when the doping ratio of **14** was increased to 1.0 wt%, the yellow emission of the obtained material exhibited a red shift, as a result of the excited state conformation changes. In addition, by choosing PEG matrices with different molecular weights, the thermochromic transition temperature of these materials could be well tuned (Fig. 13d), making them potentially useful to anti-counterfeiting and security printing.

Fig. 14 shows an example of thermo-responsive Cd(II) complex **15**, $Cd(Sal)_4(PyNH_2)_2$ (Sal = 2-formylphenolato, $PyNH_2$ = 4-aminopyridine), reported by Miao, Nie, and coworkers.[103] The crystalline **15** showed white emission at rt. Upon grinding, it was transformed into a green-emissive solid. This amorphous solid displayed thermo-sensitive luminescent changes from green at rt to yellow upon heating to 180 °C. These multi-step emission changes of **15** were mainly attributed to the effective phase transformation in the solid state rather than the change of the molecular structure. Remarkably, the plot of color temperature of emission *versus* the absolute temperature recorded from 323 to 453 K indicated a good linear relationship with a maximum relative sensitivity (S_r) of 0.95% K^{-1} at 453 K. This demonstrated that complex **15** can be used as an accurate and sensitive solid luminescent thermometer.

3.4 Metal complexes with other electronic configurations

In addition to d^6, d^8, and d^{10} complexes discussed above and the lanthanide complexes discussed below, luminescent metal complexes with other electronic configurations have been less developed. This is partially limited by the poor emitting properties of complexes with other electronic configurations. However, recent research endeavours have been able to access emissive complexes with d^3 and d^5 complexes by ligand design and some of them display interesting thermochromic properties. For example, d^3 Cr(III) complex **16** with two *N*,*N*′-dimethyl-*N*,*N*′-dipyridin-2-yl-pyridin-2,6-diamine ligands has been prepared by Heinze and coworkers, which features strong dual emissions at 775 and 739 nm with a Φ of 11%, originated from the metal-centered $^2E \rightarrow {}^4A_2$ and $^2T_1 \rightarrow {}^4A_2$ transition, respectively (Fig. 15).[104] This complex can be used as a ratiometric luminescent thermometer in the dispersion or aggregate state within a wide temperature range of 210–373 K. In the case of the dispersed sample in H_2O, upon heating from 278 to 358 K, a gradual decrease of the lower-energy emission of 775 nm and a concomitant increase of the higher-energy emission of 739 nm were observed. The Boltzmann fitting plot of the logarithm intensity ratio of the dual emissions, $\ln(I_{738}/I_{775})$, *versus* the inverse temperature T^{-1} exhibited a good linear relationship (Fig. 15b).

Recently, the research on the development of the earth-abundant d^5 Mn(II) complexes and coordination polymers has received increasing attention. A series of organic–inorganic hybrid Mn(II) complexes with three bidentate phosphine oxide ligands, represented by complex **17** in Fig. 16, have been prepared by Artem'ev and coworkers.[105a] Complex **17** possesses

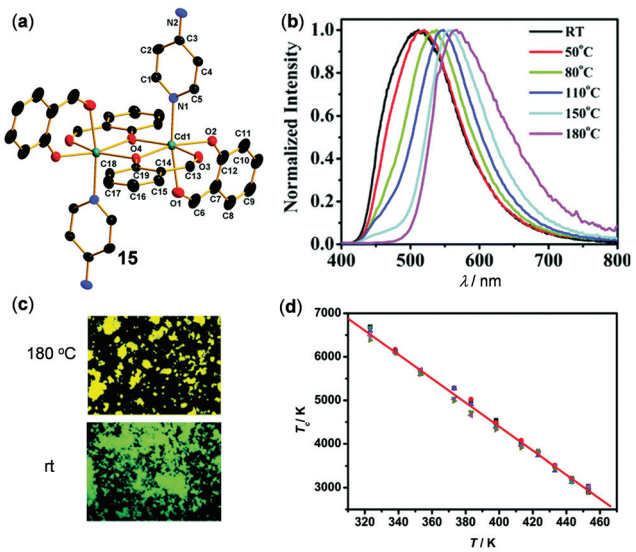

Fig. 14 (a) Single crystal structure of Cd(II) complex **15**. (b) Temperature-dependent emission spectral changes of amorphous **15** in the range of 25–180 °C. (c) Photographs showing the emission color change of **15** at rt *vs.* 180 °C. (d) The linear relationship (R^2 = 0.997) of color temperature (T_c) *versus* heating temperature (T). Reprinted with permission from ref. 103. Copyright 2019 The Royal Society of Chemistry.

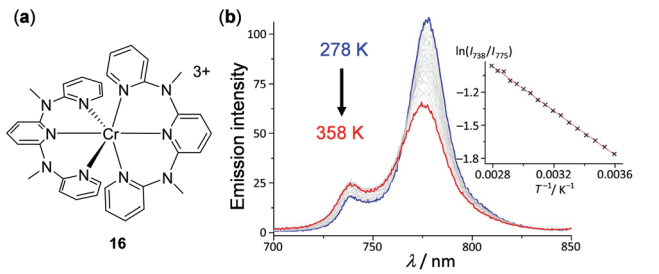

Fig. 15 (a) Molecular structure of Cr(III) complex **16** with BF_4^- counter anions. (b) Temperature-dependent emission spectra of **16** in air-saturated H_2O from 278 to 358 K. Inset: The related Boltzmann fitting plots of $\ln(I_{738}/I_{775})$ *vs.* T^{-1}. The emission changes are reversible. Reprinted with permission from ref. 104. Copyright 2017 Wiley-VCH.

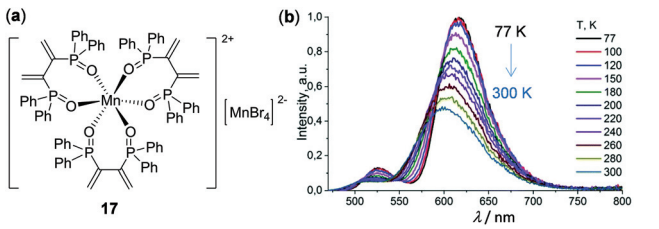

Fig. 16 (a) Molecular structure of Mn(II) complex **17**. (b) Temperature-dependent solid-state emission spectra of **17** under excitation at 440 nm in the range of 77–300 K. Reprinted with permission from ref. 105*a*. Copyright 2018 The Royal Society of Chemistry.

two different coordination models of Mn(II), *i.e.* the octahedral coordination of the $[MnO_6]^{2+}$ component and the tetrahedral geometry of the $[MnBr_4]^{2-}$ counteranion. Upon photoexcitation at 440 nm, it exhibited distinguished dual emissions at 620 and 520 nm with a high total quantum yield of 61% and a lifetime of 12–15 ms. These two emissions are assigned to different metal-centered transitions in octahedral $[MnO_6]^{2+}$ and tetrahedral $[MnBr_4]^{2-}$, respectively. As displayed in Fig. 16b, it showed distinct thermochromic luminescence induced by the dynamic thermal equilibrium of two metal-centered transitions. In addition to discrete complexes, thermochromic Mn(II) clusters or coordination polymers have been known based on single-crystal to single-crystal transformations.[105b]

3.5 Lanthanide complexes

Lanthanide complexes are important luminescent materials that have been widely applied in various optoelectronic fields. The narrow 4f–4f emission bands and long emission lifetimes of lanthanide complexes are advantageous for temperature sensing and imaging.[4] The temperature-sensing ability of a green luminescent Tb(III) complex associated with a back energy transfer from the excited state of Tb(III) $^5D_4$ to the triplet ligand-centered state has been known since 2004.[106] Using a similar strategy, a luminescent film based on a mesogenic Tb(III)-diketonate complex **18** has been recently fabricated by Lapaev and coworkers, which exhibited highly-sensitive and reversible temperature-dependent luminescence (Fig. 17).[107] Upon cooling from 284 to 143 K, the characteristic multiple emissions corresponding to the $^5D_4 \rightarrow {}^7F_J$ (J = 6–3) transitions of the ligand-to-metal energy transfer Tb(III) complex were dramatically enhanced, with a mean relative temperature sensitivity of −1.0% K^{-1}. Furthermore, the average luminescence decay time of this film also showed a distinct temperature dependence, with an absolute and relative mean temperature sensitivity of −3.3 μs K^{-1} and −0.9% K^{-1}, respectively. This demonstrates that complex **18** is a potential thermometer on the basis of both emission intensity and lifetime readouts.

Tb(III) complexes are typically green emissive. In contrast, the constructions of red or near-infrared (NIR) emissive thermometers are advantageous in bioapplications due to the high transparency of red and NIR lights in biological tissues. In this context, NIR luminescent Yb(III) complexes with distinct thermosensitive properties have been demonstrated.[108] In addition, highly red-emissive Eu(III) complexes have been reported as luminescent molecular thermometers by a few groups.[108–110] Hasegawa and coworkers recently have prepared the mononuclear Eu(III) complex **19** with bright LMCT red emissions (Fig. 18a and b).[109] Due to its steric coordination structure and dipole–dipole interactions, complex **19** displayed high thermal stability. Even at a temperature as high as 500 K, bright emission can still be observed. Moreover, complex **19** showed highly temperature-dependent emission lifetimes in a broad temperature range of 300–500 K with a relative sensitivity of −0.62% K^{-1}, making it a good candidate for temperature-sensitive paints in aerospace applications. Recently, one type of stable nanothermometer based on the thermo-responsive Eu(III) complex **20** has been prepared by Tunik and coworkers (Fig. 18c and d).[111] Complex **20** in toluene displayed a highly reversible temperature-dependent luminescence and excited-state lifetime in the physiological temperature range of 30–50 °C. The nanothermometer was fabricated by encapsulation of **20** into the assembled nanoparticle copolymer of butyl and methyl methacrylates, which showed mono-exponential lifetime decay with a relative sensitivity of 0.84% K^{-1} and a temperature resolution of 0.26 K in the presence of human serum albumin (HAS). This work provides a good nanothermometer candidate for biological applications. Beyond these results, a vitrified film of an anisometric Eu(II) β-diketone complex has been recently reported as a reusable luminescent temperature probe with excellent sensitivity in the range of 270–370 K.[110]

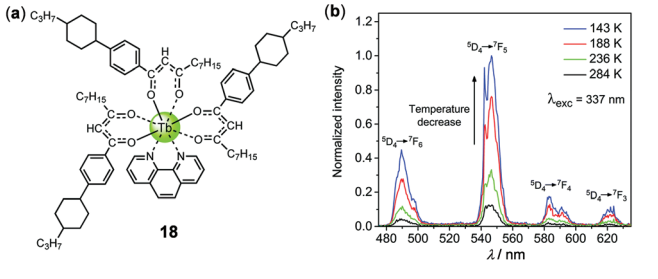

Fig. 17 (a) Molecular structure of Tb(III) complex **18**. (b) Temperature-dependent time-delayed emission spectra of a film with a time delay of 2.5 μs. Reprinted with permission from ref. 107. Copyright 2018 The Royal Society of Chemistry.

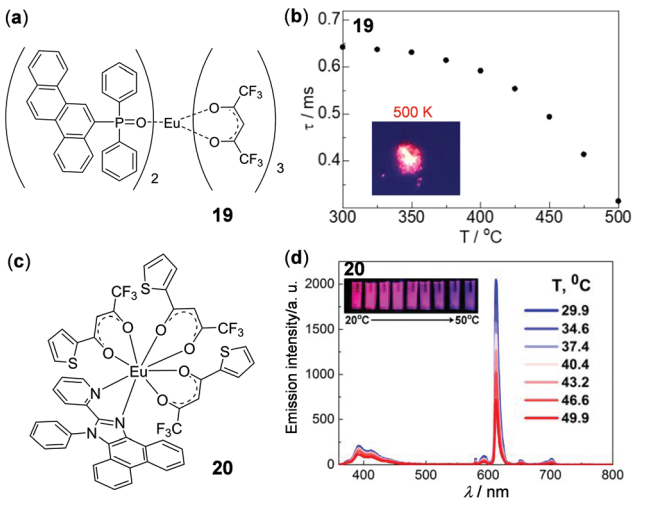

Fig. 18 (a) Molecular structure of Eu(III) complex **19**. (b) Plot of emission lifetime of **19** *versus* temperature monitored from 300 to 500 K. Inset: Photograph showing solid bright emission of **19** at 500 K. Reprinted with permission from ref. 109. Copyright 2020 American Chemical Society. (c) Molecular structure of Eu(III) complex **20**. (d) Temperature-dependent emission spectra of **20** in toluene. Inset: Emission color changes upon heating from 20 to 50 °C. Reprinted with permission from ref. 111. Copyright 2020 American Chemical Society.

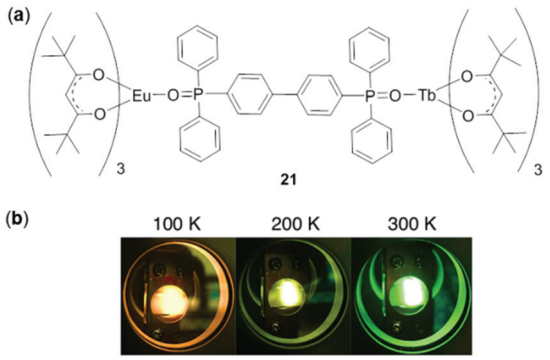

Fig. 19 (a) Molecular structure of the Eu/Tb hetero-dimetallic complex **21**. (b) Photographs showing emission colors of **21** at 100, 200, and 300 K, respectively. Reprinted with permission from ref. 113. Copyright 2018 Wiley-VCH.

In addition to monometallic complexes, dinuclear lanthanide complexes have been explored for temperature sensing.[112] In particular, heterodinuclear complexes are appealing for ratiometric temperature sensing by controlling the intramolecular energy transfer process. For this purpose, Hasegawa and coworkers prepared a seven-coordinated Eu(III)/Tb(III) hetero-dimetallic complex **21** bridged by a ditopic phosphine oxide ligand (Fig. 19).[113] This complex showed an unexpected red-to-green luminescence change upon increasing the temperature from 100 to 400 K. This phenomenon was attributed to the presence of a LMCT (from Eu^{III} to the tetramethylheptanedionate ligand) state. The complex functioned as a ratiometric thermometer with a relative thermal sensitivity and temperature uncertainty of 2.2% K^{-1} and 0.01 K, respectively.

4. Thermo-responsive metal clusters, coordination polymers, and MOFs

The research on luminescent organic–inorganic hybrid metal clusters and MOFs has been rapidly growing in the past few decades, and many of them display interesting thermo-responsive luminescence. These materials are mostly examined in the solid state. In comparison, the small molecular metal complexes discussed in the previous section are investigated in both the solution and solid states. By judicious choice of metal centers and organic ligands of various geometries and functionalities, CPs and MOFs provide an appealing platform for the development of thermo-responsive solid materials, which have been the topics of a few reviews.[3,11] We highlight herein some representative works reported in recent years.

4.1 Organic–inorganic hybrid clusters

Copper(I) halide clusters are particularly attractive materials owing to their large variety of photophysical properties associated with an extraordinary structural diversity.[114,115] On the basis of a low-energy triplet cluster-centered (^{3}CC) or halide to copper charge transfer (^{3}XMCT) transition at rt and a high-energy triplet halide-to-ligand charge transfer (^{3}XLCT) or ^{3}MLCT transition at low temperatures, a series of thermochromic luminescent materials have been developed in recent years.[3] Two examples in this context are shown in Fig. 20. Perruchas and coworkers prepared the cubane Cu_4I_4 cluster **22**, which exhibited temperature-dependent dual emissions (Fig. 20a and b).[116] At higher temperatures above 110 °C, the low-energy ^{3}CC emission at 520 nm was almost completely quenched and the high-energy emission at 400 nm caused by the intrinsic emission of the cyanobiphenyl unit was dominant. As the temperature gradually decreased to −150 °C, the ^{3}CC emission progressively enhanced, accompanied by the emission color change from deep blue to cyan. Shown in Fig. 20c and d is an octahedral Cu_4I_4 cluster (**23**) recently reported by Kolesnikov and coworkers.[117] It showed dual emissions which were both considered to be of ^{3}(X + M)LCT character. Interestingly, with an increase of the temperature from −175 to 125 °C, both emissions at 505 and 621 nm were thermally quenched albeit with different degrees of quenching. Using **23** as a sensitive thermometer, a relative thermal sensitivity of 0.12% K^{-1} at 24 °C was determined, which is comparable to the best well-known ratiometric luminescent thermometers.

In addition to Cu_4I_4 clusters, other copper(I) halide clusters have been reported to show interesting thermo-sensitive properties. For instance, a supramolecular $Cu_2I_2(NH_3)_2$-sandwiched Cu_3(pyrazolate)$_3$ adduct **24** stabilized by multiple inter-

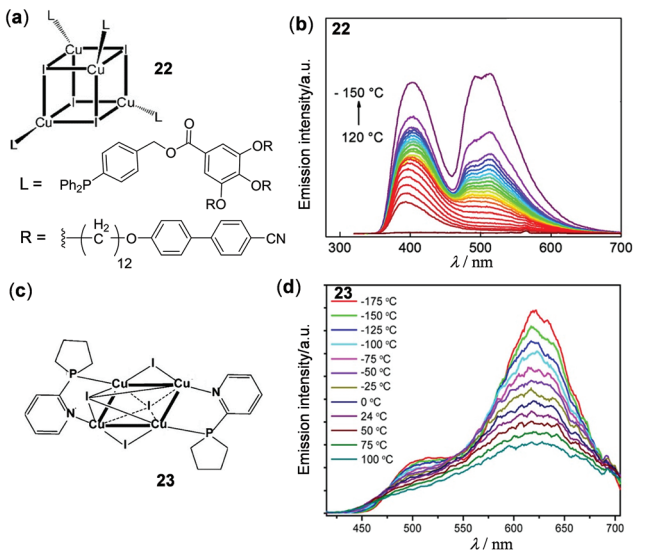

Fig. 20 (a) Chemical structure of the cubane-like Cu_4–I_4 cluster **22**. (b) Temperature-dependent emission spectra of **22** within the temperature range between −150 and 120 °C (λ_{ex} = 280 nm). Reprinted with permission from ref. 116. Copyright 2016 American Chemical Society. (c) Chemical structure of the octahedral Cu_4–I_4 cluster **23**. (d) Temperature-dependent emission spectra of **23** recorded from −175 to 100 °C. Reprinted with permission from ref. 117. Copyright 2019 American Chemical Society.

molecular $Cu_3\cdots I$, $Cu\cdots Cu$, and $N\cdots H$ interactions was reported by Zhan, Li, and coworkers as a temperature sensor (Fig. 21a and b).[118] Upon cooling from 340 to 50 K, the ^3CC emission of the solid Cu_8I_2 cluster at 590 nm was linearly enhanced with a relative sensitivity of $-0.685\%\ K^{-1}$. At around the same time, an unusual $[I@Cu_8(HMTZ)(MTZ)_7]$ (HMTZ = 1-{2-(*N*,*N*-dimethylamino)ethyl}-5-mercapto-1*H*-tetrazole) Cu(I) cluster **25** was reported to show reversible temperature-dependent dual emissions (Fig. 21c and d).[119] At rt, the powder of **25** exhibited a red emission band at 724 nm (τ = 268 ns, Φ = 3.7%) with a weak shoulder green emission band at 512 nm (τ = 32.3 ns). Upon cooling from 300 to 80 K, the green emission of **25** was enhanced much faster than the red one, causing the emission color to change from red to orange, yellow, and green, successively. As a promising ratiometric thermometer, the emission intensity ratio between 512 and 724 nm was found to display a linear relationship in the range of 80–150 K with a relative sensitivity of $8.98\%\ K^{-1}$ and a power function relation in the range of 150–250 K with a relative sensitivity of $8.32\%\ K^{-1}$.

Luminescent Ag(I) and Au(I) clusters have also received attention as solid thermo-responsive materials. For example, a Ag–S hybrid supertetrahedral cluster **26** with a discrete zero-dimensional V3,4-type structure has been constructed by Sun and coworkers (Fig. 22).[76] This material showed highly-sensitive temperature-dependent luminescence. The solid of **26** is only weakly emissive at rt. Upon cooling to 80 K, it displayed brightly yellow ^{3}LMCT emission at around 570 nm. The maximum emission peak at 180 K is slightly blue-shifted with respect to that at rt, possibly induced by the restricted peripheral pyridyl/phenyl rotation upon cooling. Additionally, the good linear relationship of maximum emission intensity *versus* temperature in the range of 80–180 K made **26** a good thermometer candidate in the low-temperature region.

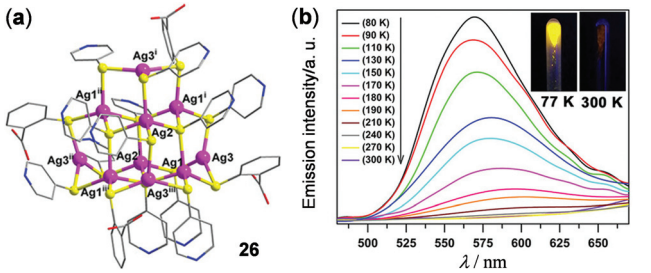

Fig. 22 (a) Crystal structure of the Ag–S hybrid cluster **26**. (b) Temperature-dependent luminescence spectra of **26** in the solid state within the temperature range of 90–300 K. Inset: Photographs showing the emission color of **26** at 77 and 300 K under 365 nm irradiation. Reprinted with permission from ref. 76. Copyright 2017 Wiley-VCH.

The above clusters are used as solid materials to sense temperature. In contrast, ultra bright luminescent Au nanoclusters (NCs) are in particular useful in various biomedical applications owing to their small size and good photostability and biocompatibility.[120,121] In a recent example, Sarkar and coworkers reported the 6-aza-2-thiothymine/L-arginine stabilized Au NCs **27** with an average diameter of 1.5 nm for temperature-sensitive applications (Fig. 23).[122] Upon heating from 15 to 55 °C in water, the green emission at 525 nm of **27** (Φ = 30%, τ_{avg} = 46 ns) was linearly decreased without a detectable

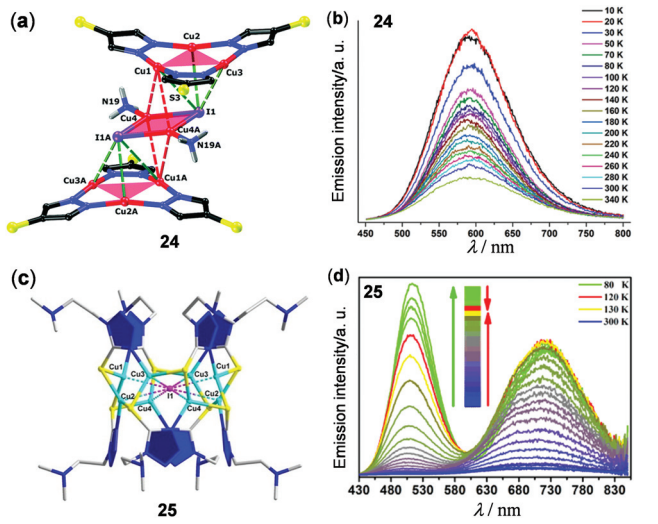

Fig. 21 (a) Crystal structure of the Cu_3–Cu_2–Cu_3 cluster **24**. (b) Temperature-dependent solid-state luminescence spectra of **24** monitored from 10 K to 340 K (λ_{ex} = 345 nm). Reprinted with permission from ref. 118. Copyright 2018 The Royal Society of Chemistry. (c) Perspective view of the $I@Cu_8$ cluster **25** viewed along the *a* axis. (d) Normalized temperature-dependent emission spectra of **25** in the solid state within the temperature range of 80–300 K. Reprinted with permission from ref. 119. Copyright 2017 American Chemical Society.

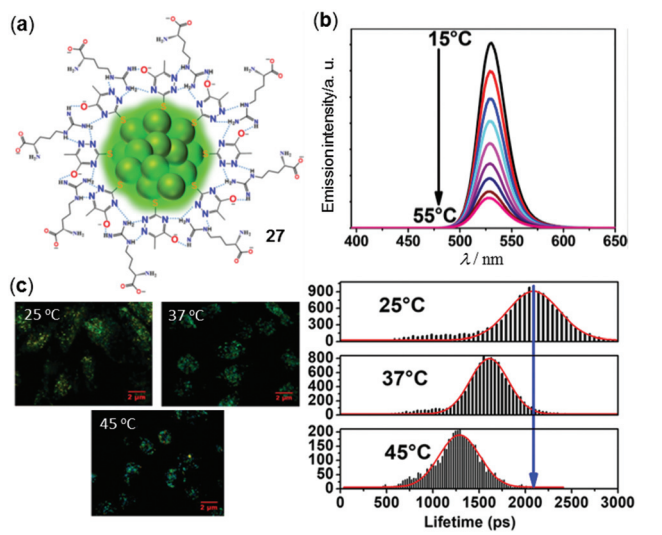

Fig. 23 (a) Chemical structural mode of Au NCs **27**. (b) Temperature-dependent emission spectra of **27** in water in the range of 15–55 °C (λ_{ex} = 375 nm). (c) Left: FLIM images of MG-63 cells with the internalized NCs **27** at 25, 37, and 45 °C. Right: Lifetime distribution histogram of intracellular NCs showing the changes in the lifetime and emission intensity at different temperatures. Reprinted with permission from ref. 122. Copyright 2019 American Chemical Society.

change of the emission maxima. Based on this phenomenon, an average sensitivity of −2.1% per °C in the physiological temperature range of 15–55 °C was calculated. Moreover, by employing the fluorescence lifetime imaging microscopy (FLIM) technique, the intracellular temperature changes of MG-63 cells with the internalized NCs **27** can be *in situ* monitored by the emission lifetime and intensity changes with high sensitivity and resolution, demonstrating the great potential of Au NCs as bio-nanothermometers (Fig. 23c).

Considering the rich luminescence properties of lanthanide complexes, metal clusters with lanthanide ions have been prepared to show thermo-responsive behaviour. Lu and coworkers prepared $Eu(III)_5$–$Ti(IV)_4$ and $Eu(III)_8$–$Ti(IV)_{10}$ clusters and found them to have temperature-sensing abilities from 180 to 240 K of 0.31% and 0.74%, respectively.[123] The temperature dependent emission response of a $Eu(III)_2$–Na_2 cluster was reported by Bruno and cowokers.[124] In addition, Wu and coworkers prepared the edge-defective cubane-like hetero-dimetallic Zn_2Ln_2 clusters **28a** and **28b** (Fig. 24).[125] By incorporation of different lanthanides, either ligand-based yellow-green emission (**28a**, Ln = Gd) or lanthanide-based red emission (**28b**, Ln = Eu) was selectively observed upon decreasing the temperature.

Recently, Calvez and coworkers reported a series of hexa-lanthanide clusters with *m*-halogenobenzoic acid ligands as solid molecular thermometric probes.[126] Shown in Fig. 25 is the structure of a hexa-Dy cluster **29**, $[Dy_6(3\text{-bb})_{14}]$ (3-bb = *m*-bromo-benzoic acid). By tuning the metal ion compositions, a series of thermochromic homo and heterodimetallic clusters have been obtained. For instance, upon cooling from 300 to 80 K, the Eu(III)-centered red emission of the $[Tb_4Eu_2(3\text{-bb})_{14}]$ cluster **30** was gradually diminished, while the green emission originated from the Tb(III)-centered excited state became dominant (Fig. 25b). These temperature-dependent emissions were

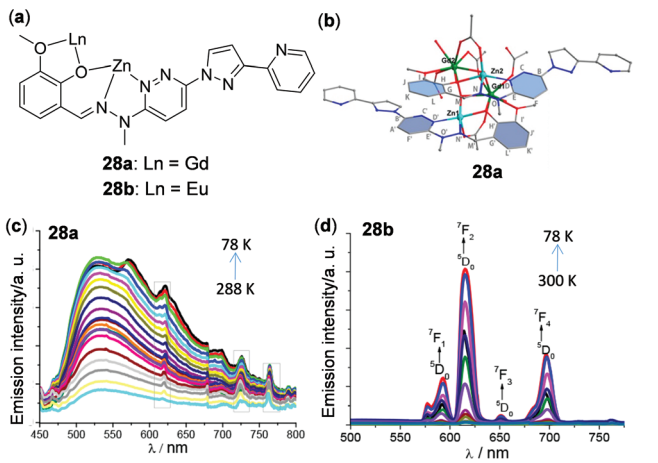

Fig. 24 (a) Structure segment of the Zn_2Ln_2 clusters **28a** and **28b**. (b) Cation core structure of **28a**. (c and d) Temperature-dependent emission spectra of (c) **28a** (78–288 K) and (d) **28b** (78–300 K) with excitation at 350 nm. The three sharp peaks marked with a gray rectangle in panel (c) are the emission spectra of a background light source. Reprinted with permission from ref. 125. Copyright 2017 American Chemical Society.

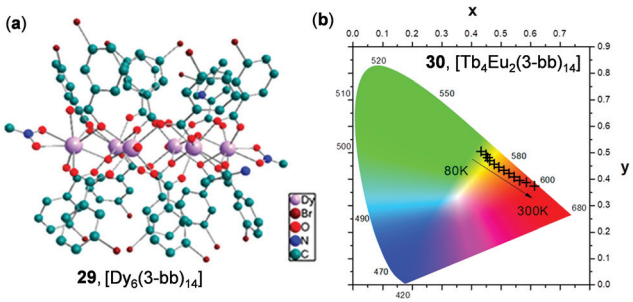

Fig. 25 (a) The core chemical structure of the Dy_6 cluster **29** (3-bb = 3-bromobenzonate). (b) Temperature-dependent CIE chromaticity coordinates of **30**, an isostructural Tb_4Eu_2 cluster, in the range of 80–300 K (λ_{ex} = 298 nm). Reprinted with permission from ref. 126. Copyright 2019 American Chemical Society.

mainly induced by the tunable ligand-involved intermetallic energy transfer.

4.2 Coordination polymers and frameworks

Luminescent CPs and frameworks have been widely investigated recently. Many of them display solid-state luminescent thermochromism. Among them, copper CPs are the focus of many research groups. One-dimensional (1D) coordination polymer **31** based on double Cu_2I_2 chains has been reported by the simple reaction of CuI and methyl 2-amino-isonicotinate by Amo-Ochoa and coworkers (Fig. 26a and b)[127] At rt, **31** is barely emissive. Upon cooling to 80 K, it exhibits bright yellow emission. The large emission enhancement was ascribed to an increase of structural rigidity. Thin film composite **31**@PVDF (4 wt%, PVDF is polyvinylidene difluoride) was subsequently fabricated, which displayed similar reversible thermochromic luminescence. Xie and coworkers prepared the Cu(I) cluster-based 1D polymer **32** from the reaction of *cis*- and *trans*-1,2-bis (4-(pyridin-2-yl)phenyl)ethane (*cis*- and *trans*-bpype) ligand with the $\{Cu_4I_4(PPh_3)_4\}$ cluster (Fig. 26c–e).[128] Polymer **32** showed reversible thermochromic dual luminescence at 516 and 640 nm. Upon cooling from 300 to 80 K, the original green emission at 516 nm, assigned to the ligand-dominated transition, was moderately enhanced. Concurrently, a new red emission band at 640 nm appeared with high intensity, causing a visual emission color change from green to red. The lower-energy red emission of **32** might be attributed to complicated charge transfer processes among Cu(I) metal sites. This study opens a new prospect for the fabrication of thermochromic luminescent CPs based on higher-nuclearity Cu(I) clusters.

In contrast to the rich structural diversity and rich photophysics of Cu(I)-halide multinuclear systems and polymers, luminescent Cu(I)-thiolate materials are less well-known. Demessence and coworkers have fabricated the two-dimensional (2D) Cu–S polymer $[Cu(p\text{-}SPhCO_2Me)]_n$ (**33**, Fig. 27).[129] This 2D sheet exhibited a simple Cu_3S_3 hexagonal tilling and half-chair conformation without direct cuprophilic interactions. Remarkably, **33** displayed intrinsic triplet emission and reversible thermochromic behavior. At a high temperature

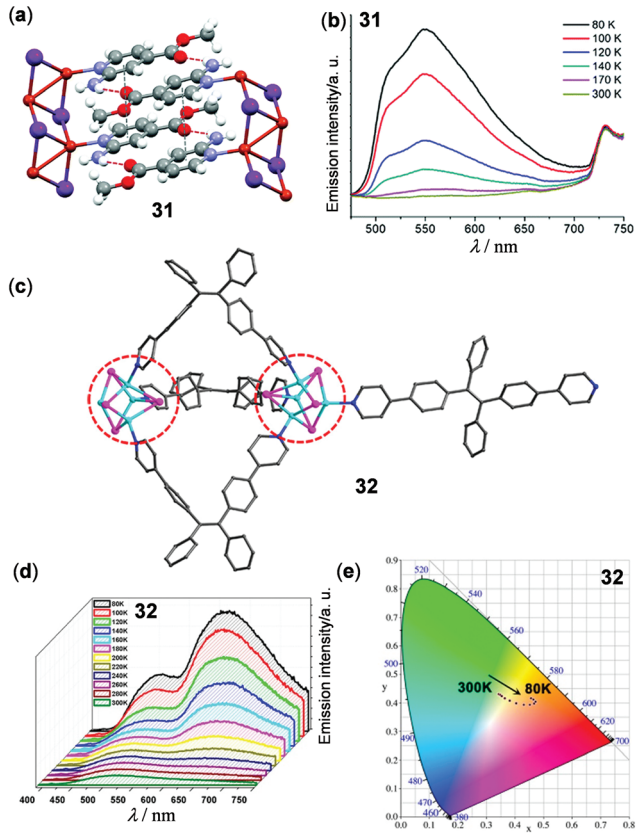

Fig. 26 (a) Crystal structure segment of the 1D Cu(I) polymer **31**. (b) Temperature-dependent solid-state emission spectra of **31** in the range of 80–300 K. Reprinted with permission from ref. 127. Copyright 2018 The Royal Society of Chemistry. (c) Asymmetric unit of the 1D Cu(I) polymer **32**. (d) Temperature-dependent solid-state emission spectra and (e) CIE chromaticity diagram of **32** in the range of 80–300 K (λ_{ex} = 380 nm). Reprinted with permission from ref. 128. Copyright 2017 American Chemical Society.

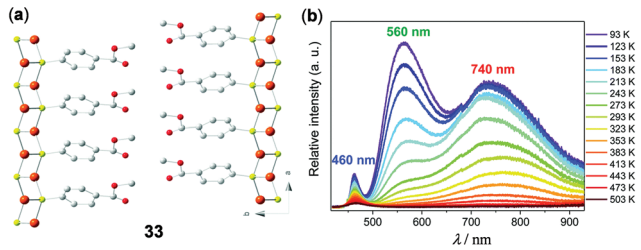

Fig. 27 (a) Structure representation of the 2D Cu–S polymer **33** viewed from the *c* axis. Orange, Cu; yellow, S; red, O; grey, C. Hydrogen atoms are omitted for clarity. (b) Temperature-dependent solid-state emission spectra of **33** between 93 and 503 K (λ_{ex} = 380 nm). Reprinted with permission from ref. 129. Copyright 2016 The Royal Society of Chemistry.

of 500 K, the material is barely emissive. Upon cooling to 93 K, two intense green and red emission bands progressively appeared at 560 and 740 nm. The maximum relative sensitivity (S_r) reached 1.37% K^{-1} at 353 K, suggesting the great potential of **33** as a ratiometric high-temperature thermometer.

In addition to 1D and 2D CPs, Cu cluster-based three-dimensional (3D) MOFs with temperature-responsive luminescent properties have been investigated. For instance, the copper halide-based 3D MOF **34**, $[Cu_6I_6Br_2C_{16}H_{32}N_4]$, has been reported by Xin and coworkers (Fig. 28).[65] MOF **34** is composed of a 2-fold interpenetrated pillared-layered framework structure with two different coordination modes of the rhombohedral Cu_2I_2 dimers with a *trans* conformation. Depending on the excitation wavelength, MOF **34** displayed different thermochromic luminescence. Under excitation at 290 nm, the two emissions at 500 and 620 nm were both significantly enhanced as the temperature decreased from 300 K down to 6 K (Fig. 28c). In contrast, under the excitation at 350 nm, a distinct shift of the maxima emission peak from 530 to 602 nm was observed (Fig. 28d). The authors deduced that this difference was caused by the different magnitudes of structural changes of two Cu_2I_2 dimers.

Silver-chalcogenolate cluster-based MOFs are a new family of coordination luminescent materials, whose stability is enhanced by the extended network structures. In 2016, Sun and coworkers have reported the $[Ag_2(pz)(bdc)\cdot H_2O]_n$ (pz = pyrazine, and H_2bdc = benzene-1,3-dicarboxylic acid) MOF to show two-step thermo-responsive luminescence mainly induced by the single-crystal to single-crystal phase transition.[130] Two years later, Zang and coworkers reported the luminescent hydrogen-bonded pillared-layered silver MOF, $[Ag_{10}(SBu^t)_6(CF_3COO)_2(PhPO_3H)_2(bpy)_2]_n$ (**35**) to display thermochromic properties (Fig. 29).[131] MOF **35** showed typical nonradiative decay at 518 nm with increasing temperature (Fig. 29c). Interestingly, the solvent-included MOF **35**·$CHCl_3$

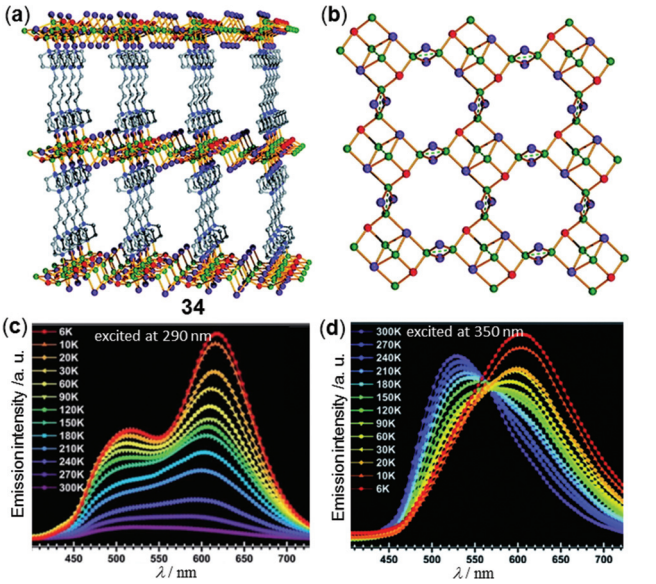

Fig. 28 (a) Independent 3D framework pillared-layered structure and (b) copper-halide single layer structure of Cu-MOF **34**. (c and d) Temperature-dependent solid-state emission spectral changes of **34** in the range of 6–300 K excited at (c) 290 nm or (d) 350 nm. Reprinted with permission from ref. 65. Copyright 2018 The Royal Society of Chemistry.

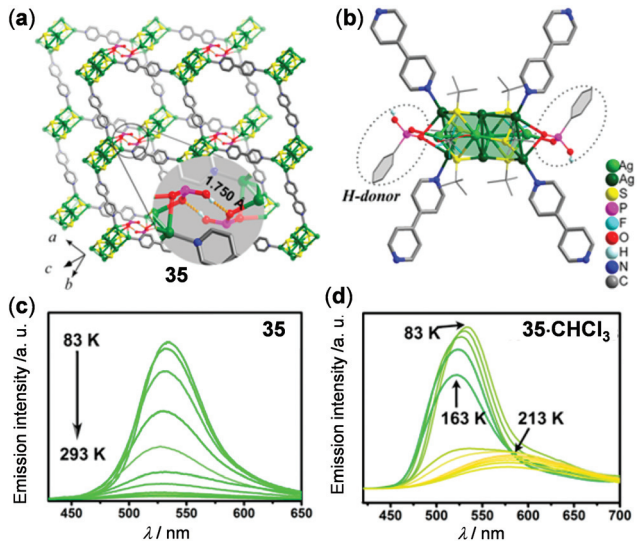

Fig. 29 (a) Two-layer stack and (b) perspective view of the coordination environment of Ag-MOF **35**. (c and d) Temperature-dependent solid-state emission spectral change of (c) **35** and (d) **35**·$CHCl_3$. Reprinted with permission from ref. 131. Copyright 2018 American Chemical Society.

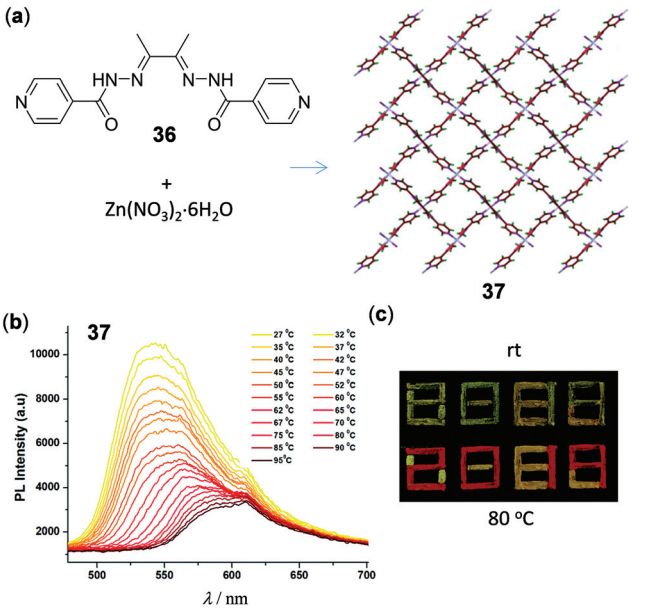

Fig. 30 (a) Schematic representation of the synthesis of 2D Zn(II) polymer **37**. (b) Temperature-dependent solid-state emission spectra of **37** in the range of 27–95 °C. (c) Photographs under UV irradiation of **37** at ambient temperature and 80 °C, respectively. Reprinted with permission from ref. 133. Copyright 2020 The Royal Society of Chemistry.

displayed multistep emission spectral (534 → 522 → 579 nm) and color (green to yellow) changes upon heating from 83 to 213 K (Fig. 29d), suggesting the potential of MOF materials in modulating the thermochromic properties by host–guest chemistry.[132]

In addition to Cu and Ag materials, luminescent Zn(II) polymers and MOFs have been shown to possess interesting thermochromic properties. A recent report by Tom and coworkers presented the 2D layered Zn(II) polymer **37**, which was prepared from $Zn(NO_3)_2$ with the 2,3-butanedionebisisonicotinylhydrazone ligand **36** (Fig. 30).[133] Polymer **37** is characterized by a 4-connected unimodal 2D layered framework and reversible temperature-dependent luminescence. Upon heating from 30 to 100 °C, the intense LMCT yellow emission at 550 nm of **37** shifted progressively to 600 nm with a partial decrease of the emission intensity. This phenomenon was induced by the proposition of fast dehydration/hydration processes without alternation of the crystal structure of **37**. Polymer **37** could be used as a wavelength- and intensity-based thermometer with a maximum relative sensitivity of 0.02% at 45 °C and 0.04% at 70 °C, respectively. As a demonstration in document security application, the patterned security feature of "2019" encrypted with thermochromic **37** could be readily visualized in red emission colors upon heating to 80 °C (Fig. 30c).

As an example of 3D thermo-responsive luminescent Zn(II) MOFs, a mixed-ligand MOF ZnATZ-BTB (ATZ = 5-amino-1-*H*-tetrazolate, BTB = 1,3,5-tris(4-carboxyphenyl)-benzene) has been constructed by Wu and coworkers to function as a ratiometric thermometer at cryogenic temperatures.[134] In addition, based on the dual emissive 5-(2-(5-fluoro-2-hydroxyphenyl)-4,5-bis(4-fluorophenyl)-1*H*-imidazol-1-yl)isophthalic acid ligand **38** (H_2hpi_2cf) with the characteristic excited state intramolecular proton transfer (ESIPT) properties, a robust microporous (<3 Å) Zn(II) MOF **39**, $Zn(hpi_2cf)(DMF)(H_2O)$, with temperature-dependent luminescence was fabricated by Su, Pan, and coworkers (Fig. 31).[135] Upon heating or cooling, green and blue emissions of **39** were reversibly switched, in which the ESIPT process triggered by the interconversion of hydrated and dehydrated crystalline phases was proposed to play a significant role. Subsequently, ZnO-supported hybrid films based on **39** were prepared, which exhibited potential applications in the detection of trace water (<0.05%, v/v) and thermal imaging (Fig. 31c). Apart from these results, Yan and coworkers recently constructed a Zn_5-cluster based MOF with 5-bromoisophthalic acid and 2-methylimidazole mixed ligands to show temperature-responsive dual fluorescence and room temperature phosphorescence.[136] Li and coworkers have fabricated a series of dye–MOF composites by employing the biocompatible Zn(II) MOF, Zn_3(benzene-1,3,5-tricarboxyl)$_2$(adenine)(H_2O) as a host and different thermo-sensitive organic dyes as guests.[137] By making full use of the energy transfer between the frameworks and incubated dyes, highly sensitive and reversible ratiometric thermometers were realized under physiological cellular conditions.

Similar to the small molecular lanthanide complexes, lanthanide CPs and MOFs are characterized by strong and narrow solid-state emissions with long lifetimes. The applications of lanthanide CPs and MOFs in temperature sensing have been well-established.[138–140] In a classical example, Zhou and coworkers reported the isostructural lanthanide MOF $(Me_2NH_2)_3[Eu_3(FDC)_4(NO_3)_4]\cdot 4H_2O$ (H_2FDC = 9-fluorenone-2,7-dicarboxylic acid) to display ratiometric temperature sensing

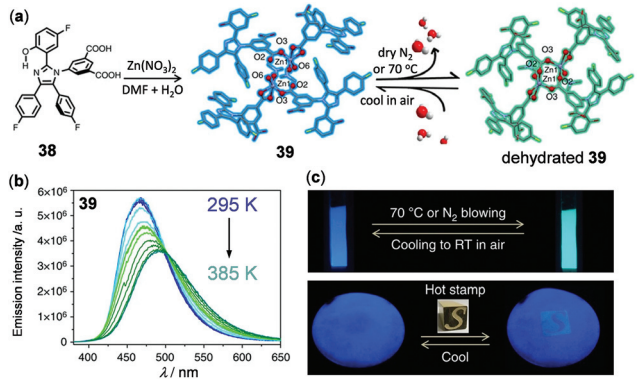

Fig. 31 (a) Schematic diagram showing the synthetic route and structural transformation of Zn MOF **39**. (b) Temperature-dependent emission spectral changes of **39** microcrystals. (c) Photographs showing the thermochromic applications of the ZnO-supporting hybrid film of **39**. Up: Blue and green emission color switching upon heating/N_2 blowing and cooling. Below: Thermal imaging using a heated stone seal of 100 °C on the paper film. Reprinted with permission from ref. 135. Copyright 2017 Nature.

over a wide temperature range (12–320 K) with a high maximum relative sensitivity of 2.3% K^{-1} at 140 K.[141] In addition, a single phosphonate-based MOF **40**, [Tb(H_5btp)]·2H_2O [H_8btp = (1,1′-biphenyl)-3,3′,5,5′-tetrayltetrakis (phosphonic acid)], was disclosed by Rocha and coworkers (Fig. 32).[142] MOF **40** contained an uncommon slightly distorted {TbO_6} octahedron and lozenge-shaped tubular channels through intermolecular π–π interactions (d = 3.856 Å) of adjacent biphenyl ligands. Upon heating from 299 to 319 K, the ligand-centered emission at 316–386 nm, the ligand-associated excimer emission at 390–476 nm, and the $^5D_4 \rightarrow {}^7F_5$ emission of Tb(III) at 490–560 nm all decreased linearly as a function of temperature, with the maximum relative errors of 1% at 313 K, 1.3% at 299 K, and 0.4% at 301 K, respectively.

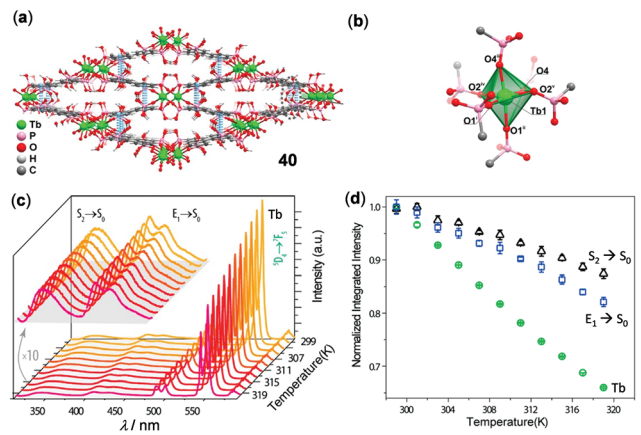

Fig. 32 (a) Crystal packing network and (b) Tb(III) octahedral coordination environment of Tb MOF **40**. (c) Temperature-dependent solid-state emission spectral change of **40** in the range of 299–319 K (λ_{ex} = 300 nm). (d) Temperature dependence of integrated intensities of different emissions. Reprinted with permission from ref. 142. Copyright 2017 American Chemical Society.

In addition to homometallic CPs or MOFs, a number of lanthanide coordination materials with two different metal ions have been reported for the purpose of ratiometric temperature sensing. In a classical example, Hasegawa reported the color-changeable Tb(III)/Eu(III) mixed 1D CPs, bridged by a ditopic phosphine oxide ligand, to display highly sensitive ratiometric temperature sensing over a wide range (200–500 K).[143] Recently, phenanthroline 1D CPs grafted with Eu(III) and Tb(III) trifluoactylacetone (tfac) complexes have been reported as a noncontact temperature sensor in the range of 260–460 K.[144] Based on the energy transfer mechanism, Zaręba and coworkers reported the Eu/Tb-co-doped 2D CPs **41** with good three-photon absorption capability, which could be used as a NIR-to-VIS ratiometric luminescent thermometer under the excitation of NIR light (Fig. 33).[145] Polymer **41** exhibited a 2D, three-connected coordination network with a honeycomb-like layer. More interestingly, under the three-photon excitation at 800 nm, the emission of **41** showed a

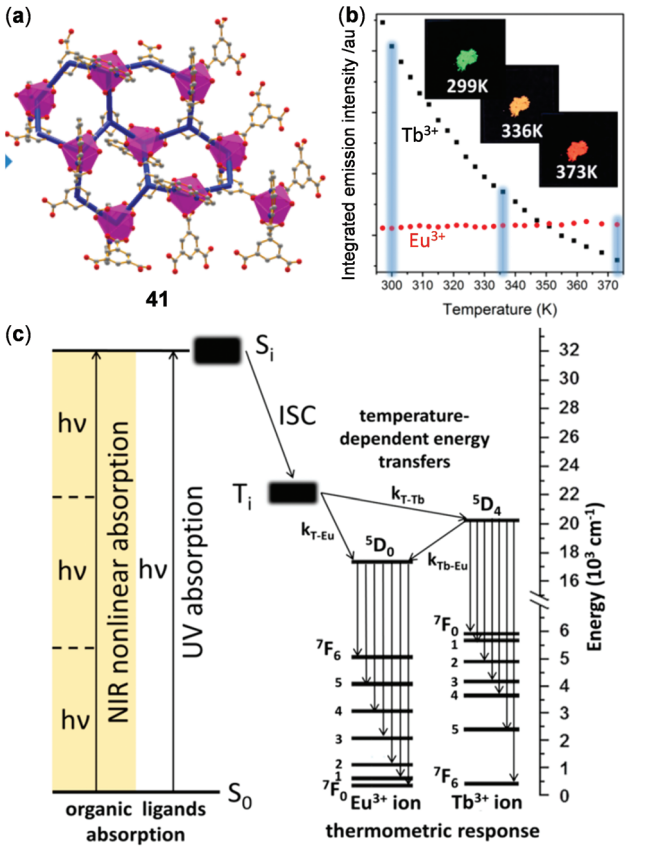

Fig. 33 (a) Honeycomb-like Eu/Tb mixed 2D coordination polymer **41**. (b) Plots of the integrated intensity of $^5D_0 \rightarrow {}^7F_2$ of Eu(III) (red dots) and $^5D_4 \rightarrow {}^7F_5$ of Tb(III) (black dots) f–f emission as a function of temperature (excited at 337 nm). Insets: Photographs showing the emission color of **41** at 299, 336, and 373 K, respectively. (c) Energy level diagram highlighting the use of three-photon excitation for effecting the thermometric luminescent response. Reprinted with permission from ref. 145. Copyright 2019 American Chemical Society.

similar temperature-dependency of emission in the range of 299–373 K with respect to that under one-photon excitation at 337 nm. Upon heating from 299 K to 373 K, the green emission of the $^5D_4 \rightarrow {}^7F_5$ transition of Tb(III) dropped abruptly while the red emission of the $^5D_0 \rightarrow {}^7F_2$ excited state of Eu(III) increased slightly, in accompany with an obvious solid emission color change from green to red. The relative sensitivity under the three-photon excitation at 800 nm was calculated to be 2.91% K^{-1}, demonstrating the possibility of NIR light-excited optical thermosensing.

In the case of thermo-sensitive Tb(III)/Eu(III) mixed 3D MOFs, the first report was given by Qian and coworkers.[73] Stimulated by this study, a great number of mixed MOFs have been fabricated for the purpose of temperature sensing.[11] Two of the recently reported examples are highlighted below. Zhao, Qian, and coworkers reported the Eu/Tb mixed MOF **42**, $Eu_{0.05}Tb_{0.95}$FTPTC (H_4FTPTC = 2′-fluoro-[1,1′:4′,1″-terphenyl]-3,3″,5,5″-tetracarboxylic acid), which featured a 3D network and distorted tricapped trigonal prism coordination of Ln atoms (Fig. 34a and b).[146] As a result of the thermal-driven energy transfer from Tb(III) to Eu(III), **42** showed a reversible linear response to temperature with high relative sensitivity (9.11% K^{-1} at 125 K) in the cryogenic range of 25–125 K. In addition, Su and coworkers synthesized the Eu(III)/Tb(III) mixed MOF **43**, $[(CH_3)_2NH_2]Eu_{0.036}Tb_{0.964}$BPTC (BPTC is the deprotonated form of biphenyl-3,3′,5,5′-tetracarboxylic acid), which showed highly-sensitive temperature-dependent ratiometric and colormetric luminescence (Fig. 34c and d).[72] Upon heating from 167 to 377 K, the emission intensity of the Tb(III) $^5D_4 \rightarrow {}^7F_5$ transition of **43** decreased by about 89%, while the emission intensity of the Eu(III) $^5D_0 \rightarrow {}^7F_2$ transition showed a 4-fold enhancement. Concurrently, the solid emission color of **43** gradually changed from green to yellow and red. The plot of the Tb/Eu emission intensity ratio *versus* temperature in the 220–310 K range displayed a good linear relationship with a high maximum relative sensitivity of 9.42% K^{-1} at 310 K.

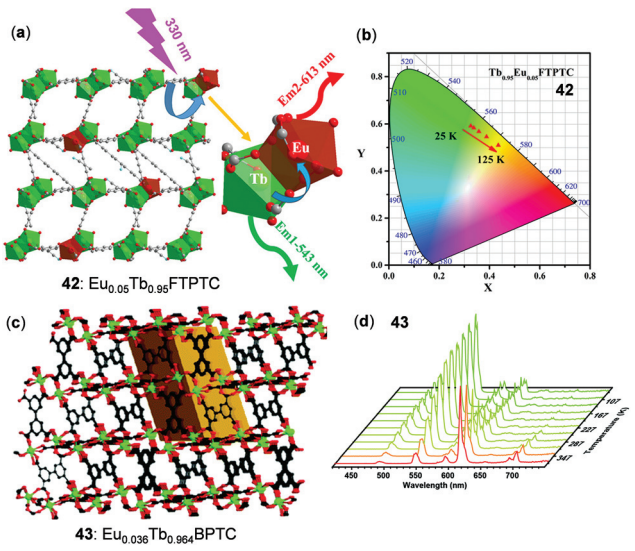

Fig. 34 (a) Schematic representation of the resonance energy transfer mechanism of MOF **42**. (b) Temperature-dependent CIE chromaticity coordinates of **42** within the range of 25–125 K (λ_{ex} = 350 nm). Reprinted with permission from ref. 146. Copyright 2018 American Chemical Society. (c) Structure of Ln-MOF **43**. (d) Temperature-dependent solid-state emission spectra of **43** between 77 and 377 K (λ_{ex} = 322 nm). Reprinted with permission from ref. 72. Copyright 2019 The Royal Society of Chemistry.

5. Multi-component coordination copolymers and assemblies

Donor–acceptor energy transfer is long known to be highly dependent on temperature. By manipulating the efficiency of energy transfer in materials containing two or more than two chromophores, distinct ratiometric luminescence changes are expected. This has been discussed in bridged dyads, heterodimetallic clusters, and mixed-metal MOFs in the previous sections (Fig. 19, 25 and 34).[113,116,146] Using a similar strategy, thermo-responsive luminescent assemblies have been developed with tuneable excited states. However, controlled energy transfer is not the only reason for the thermo-responsiveness of assembled or composite materials. Other factors such as reversible coordination/dissociation and changes in the microenvironment polarity have been utilized to fabricate thermo-responsive assemblies.

In order to utilize effective energy transfer between luminescent metal complexes and organic chromophores, Wolfbeis and coworkers presented a nanothermometer by the co-assembly of the thermo-stable blue-emissive polyfluorene **44** and the thermo-sensitive red-emissive Eu(III) complex **45** (Fig. 35).[147] In the obtained nanocomposite **46**, efficient fluorescence resonant energy transfer (FRET) from the light-harvesting polyfluorene antenna to the doped Eu(III) complex occurred. Under the two-photon excitation at 720 nm at rt, dual emissions in the blue and red region were observed. Upon heating from 270 to 320 K, both emissions decreased gradually. However, relative to the blue emission of polyfluorenes, the red Eu(III) emission dropped much faster. The fitting plot of the Eu and polyfluorene emission ratio *versus* temperature showed a good linear relationship with a relative sensitivity of 1.6% K^{-1}, suggesting its potential applications as ratiometric nanothermometers. In addition to **46**, FRET nanoparticles with the combination of other donors and acceptors are known.[148]

Recently, Zhong, Yao, and coworkers have fabricated a class of highly ordered crystalline phosphorescent nanotubes from the co-assembly of two neutral Ir(III) complexes, **47** and **48**, acting as the effective antenna chromophore and energy acceptor, respectively (Fig. 36).[149] Due to the excellent light-harvesting and energy transfer process, the phosphorescence color of these nanotubes was finely tuned from green to red by varying temperature. Upon cooling from 298 to 77 K, the red emission of these nanotubes containing 0.06% of acceptor was gradually turned green, which was caused by the inhibited energy transfer at low temperatures.

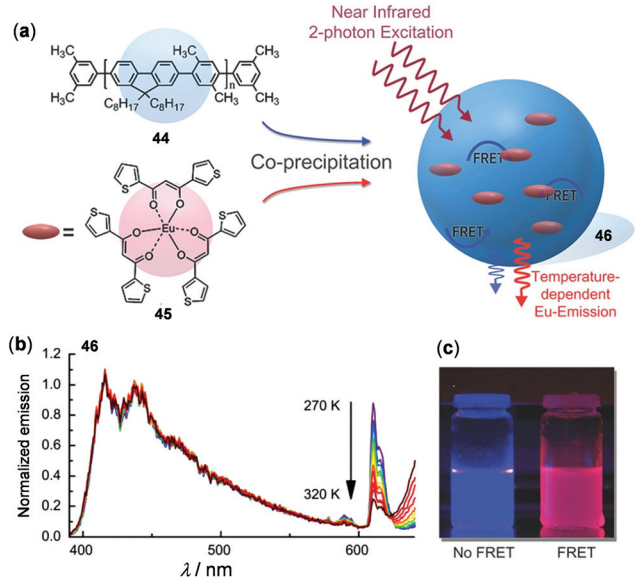

Fig. 35 (a) Molecular structures of **44** and **45** and schematic illustration showing the mechanism of the FRET-based nano-thermometer of the binary-assembled composite **46**. (b) Normalized temperature-dependent emission spectra of **46** with two-photon excitation (λ_{ex} = 720 nm). (c) Photographs exhibiting the emission color change of the nanoparticles before (left) and after precipitation (right) in water under UV irradiation. Reprinted with permission from ref. 147. Copyright 2016 WILEY-VCH.

As an example of thermo-responsive assembled or composite materials that are not based on the energy transfer mechanism, Li and coworkers reported a ratiometric luminescent thermometer through the combination of the Eu(III) complex **50** and the Zn(II) complex **51** prepared from the same tridentate ligand **49** (Fig. 37).[150] The composite material **52** was obtained from two individual complexes in a 1 : 19 molar ratio. Upon cooling from 500 to 80 K, the red Eu(III) emission of **52** increased dramatically, whereas the blue emission associated with the Zn(II) component showed a little change. Based on this, a good linear relationship between two emission intensities was observed from 80 to 410 K with a temperature sensitivity of 0.896% K^{-1}. The excellent thermo-responsiveness of **52** was considered to be mainly attributed to the dynamic coordination (at low temperatures) and dissociation (at higher temperatures) of the Eu(III) component. However, temperature had little effect on the Zn(II) component and it simply behaved as an internal reference for the ratiometric sensing. No intermetallic energy transfer between Eu(III) and Zn(II) was involved in this system.

The combination of two or more chromophores through copolymerization is another appealing strategy to construct ratiometric luminescent thermo-responsive materials. Zhao, Huang, and coworkers prepared copolymer **53** by introducing two different Ir(III) complexes into the thermosensitive poly *N*-isopropylacrylamide backbone for the *in vitro* and *in vivo* temperature sensing and imaging (Fig. 38).[151] Upon increasing temperature, this polymer underwent a coil–globule transition, leading to a decrease in microenvironment polarity surround-

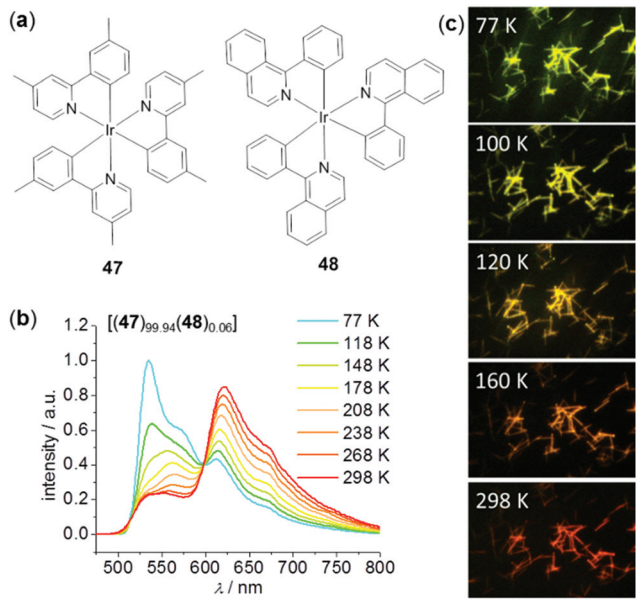

Fig. 36 (a) Molecular structures of donor **47** and acceptor **48**. (b) Temperature-dependent emission spectra of nanotube **47** doped with 0.06% of **48** (λ_{ex} = 375 nm). (c) Fluorescence microscopy images displaying the temperature-dependent emission color changes of the doped nanotubes. Reprinted with permission from ref. 149. Copyright 2018 Wiley-VCH.

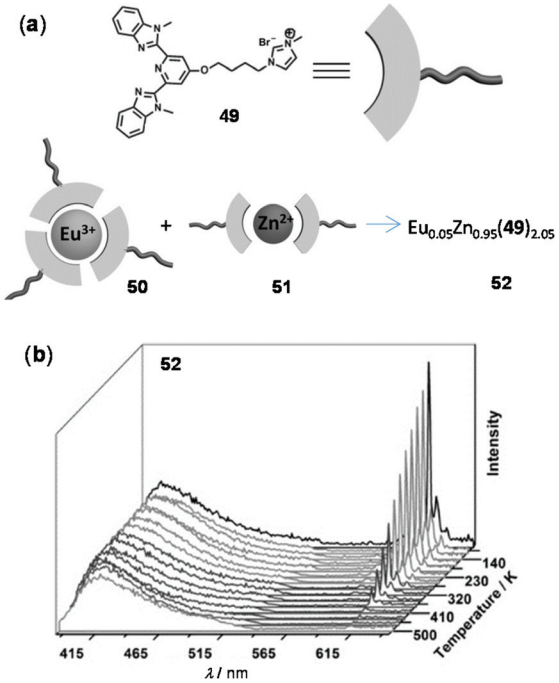

Fig. 37 (a) Molecular structures of **49**–**52**. (b) Temperature-dependent emission spectra of **52** recorded from 80 to 500 K. Reprinted with permission from ref. 150. Copyright 2015 Wiley-VCH.

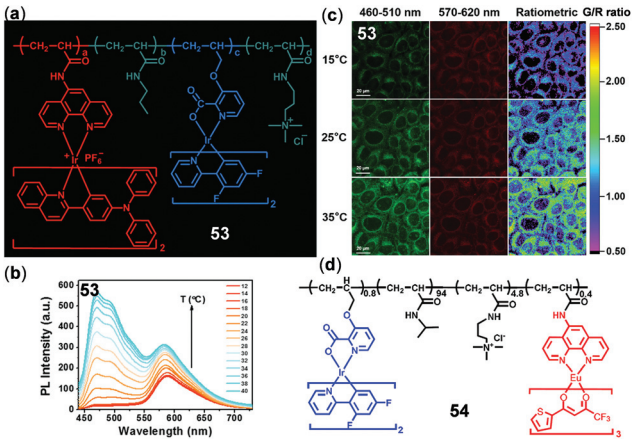

Fig. 38 (a) Chemical structure of copolymer **53** (a/b/c/d = 0.11/100/0.89/2.32). (b) Temperature-dependent emission spectra of **53** (0.01 w/v%) in PBS buffer (12–40 °C). (c) Confocal laser scanning microscopy images of HeLa cells labelled with **53** at 15 °C (top), 25 °C (middle), and 35 °C (bottom). Reprinted with permission from ref. 151. Copyright 2016 WILEY-VCH. (d) Chemical structure of copolymer **54**. Reprinted with permission from ref. 79. Copyright 2018 American Chemical Society.

ing the Ir(III) complexes and hence enhanced the emissions of both Ir(III) complexes. However, owing to the different sensitivity to the surrounding environment, the green/red emission intensity ratio was linearly correlated with temperature. Thus, polymer **53** has been successfully used for temperature sensing and imaging of HeLa cells (Fig. 38c) and zebrafish. Recently, the same research group reported another copolymer **54** containing a green emissive Ir(III) component and a red emissive Eu(III) component (Fig. 38d).[79] In addition to the application as a ratiometric temperature probe in the physiological temperature range, polymer **54** also exhibited a high temperature-dependence of excited state lifetimes, making it applicable for temperature-dependent ratiometric luminescence imaging and phosphorescent lifetime imaging in biological systems.

6. Conclusion

In summary, this review provides the fundamentals and design strategies for the development of thermo-responsive metal–ligand coordination materials. The thermo-responsiveness is commonly read out by the signal changes in the emission intensity, maximum emission wavelength, or excited-state lifetime, with more than one parameter changes being involved in many systems. This temperature-responsiveness could be caused by the thermal-activated non-radiative transition, the thermal equilibrium of different excited states, molecular structural or conformation changes, the changes in molecular stacking, controlled inter-/intramolecular energy transfer, changes in the microenvironment polarity, *etc*. Ratiometric luminescence response is particularly appealing for highly-sensitive temperature sensing and imaging, which can be realized on molecular dyads, mixed-metal clusters, MOFs, host–guest systems, and binary polymers and assemblies.

Among the materials surveyed in this review, small molecular metal complexes with well-determined molecular structures are particularly useful for studies in the solution state. In addition, they could be used as building blocks to prepare thermo-responsive polymers and assemblies with tailored sizes for biomedical applications. In comparison, metal clusters and MOFs are particularly used as solid-state thermo probes owing to their high thermal stability. They could also be good candidates for applications under harsh conditions, such as cryogenic conditions or a high-temperature environment. In addition to these materials, another type of thermo-responsive luminescent material is thermally activated delayed fluorescence (TADF) compounds, which have received intense interest but not discussed in this review. We are aware that the topic of metal complex-based TADF materials, in particular Cu(I), Ag(I), Au(I) complexes, has been recently reviewed by Yersin, Li, and co-workers.[152] Although these complexes have been mainly investigated as OLED materials in the current stage, the exploitation of the thermo-responsive nature of these materials is expected to receive growing attention in the future.

Regarding the future research in this field, attention could also be paid to the preparation of non-precious earth-abundant metal complexes with distinct thermo-responsive properties, *e.g.* Cr, Mn, W complexes, and the incorporation of these complexes into more sophisticated systems. In addition, the thermo input and luminescence readout could be combined with other stimulus and readout means, such as optical, magnetic, electrical, and chemical signals to develop multifunctional intelligent systems. During the practical applications of thermo-responsive coordination materials, the material stability and robustness, that could ensure high reversibility and long-term cyclability, must be considered.

Conflicts of interest

The authors declare no conflicts of interest.

Acknowledgements

The authors acknowledge the funding support from the National Science Fund for Distinguished Young Scholars (No. 21925112), the National Natural Science Foundation of China (grants 21601194 and 21872154) and the Beijing Natural Science Foundation (grant 2191003).

Notes and references

1 X.-d. Wang, O. S. Wolfbeis and R. J. Meier, Luminescent probes and sensors for temperature, *Chem. Soc. Rev.*, 2013, **42**, 7834.

2 Y. Cui, F. Zhu, B. Chen and G. Qian, Metal–organic frameworks for luminescence thermometry, *Chem. Commun.*, 2015, **51**, 7420.
3 B. Li, H.-T. Fan, S.-Q. Zang, H.-Y. Li and L.-Y. Wang, Metal-containing crystalline luminescent thermochromic materials, *Coord. Chem. Rev.*, 2018, **377**, 307.
4 Y. Hasegawa and Y. Kitagawa, Thermo-sensitive luminescence of lanthanide complexes, clusters, coordination polymers and metal–organic frameworks with organic photosensitizers, *J. Mater. Chem. C*, 2019, **7**, 7494.
5 Y. Cheng, Y. Gao, H. Lin, F. Huang and Y. Wang, Strategy design for ratiometric luminescence thermometry: circumventing the limitation of thermally coupled levels, *J. Mater. Chem. C*, 2018, **6**, 7462.
6 E. J. McLaurin, L. R. Bradshaw and D. R. Gamelin, Dual-Emitting Nanoscale Temperature Sensors, *Chem. Mater.*, 2013, **25**, 1283.
7 P. Mahata, S. K. Mondal, D. K. Singha and P. Majee, Luminescent rare-earth-based MOFs as optical sensors, *Dalton Trans.*, 2017, **46**, 301.
8 D. Zhao, Y. Cui, Y. Yang and G. Qian, Sensing-functional luminescent metal–organic frameworks, *CrystEngComm*, 2016, **18**, 3746.
9 C. D. S. Brites, P. P. Lima, N. J. O. Silva, A. Millá, V. S. Amaral, F. Palacio and L. D. Carlos, Lanthanide-based luminescent molecular thermometers, *New J. Chem.*, 2011, **35**, 1177.
10 F.-Y. Yi, D. Chen, M.-K. Wu, L. Han and H.-L. Jiang, Chemical Sensors Based on Metal–Organic Frameworks, *ChemPlusChem*, 2016, **81**, 675.
11 L. Chen, D. Liu, J. Peng, Q. Du and H. He, Ratiometric fluorescence sensing of metal-organic frameworks: Tactics and perspectives, *Coord. Chem. Rev.*, 2020, **404**, 213113.
12 X. Zhou, H. Wang, S. Jiang, G. Xiang, X. Tang, X. Luo, L. Li and X. Zhou, Multifunctional Luminescent Material Eu(III) and Tb(III) Complexes with Pyridine-3,5-Dicarboxylic Acid Linker: Crystal Structures, Tunable Emission, Energy Transfer, and Temperature Sensing, *Inorg. Chem.*, 2019, **58**, 3780.
13 P. M. Gschwend, D. Niedbalka, L. R. H. Gerken, I. K. Herrmann and S. E. Pratsinis, Simultaneous Nanothermometry and Deep-Tissue Imaging, *Adv. Sci.*, 2020, **7**, 2000370.
14 T. Bai and N. Gu, Micro/Nanoscale Thermometry for Cellular Thermal Sensing, *Small*, 2016, **12**, 4590.
15 M. Nakano and T. Nagai, Thermometers for monitoring cellular temperature, *J. Photochem. Photobiol., C*, 2017, **30**, 2.
16 X. Hu, Y. Li, T. Liu, G. Zhang and S. Liu, Intracellular Cascade FRET for Temperature Imaging of Living Cells with Polymeric Ratiometric Fluorescent Thermometers, *ACS Appl. Mater. Interfaces*, 2015, **7**, 15551.
17 J. Dong, Y. Pan, H. Wang, K. Yang, L. Liu, Z. Qiao, Y. D. Yuan, S. B. Peh, J. Zhang, L. Shi, H. Liang, Y. Han, X. Li, J. Jiang, B. Liu and D. Zhao, Self-Assembly of Highly Stable Zirconium(IV) Coordination Cages with Aggregation Induced Emission Molecular Rotors for Live-Cell Imaging, *Angew. Chem., Int. Ed.*, 2020, **59**, 10151.
18 J. Dong, Z. Qiao, Y. Pan, S. B. Peh, Y. D. Yuan, Y. Wang, L. Zhai, H. Yuan, Y. Cheng, H. Liang, B. Liu and D. Zhao, Encapsulation and Protection of Ultrathin Two-Dimensional Porous Organic Nanosheets within Biocompatible Metal–Organic Frameworks for Live-Cell Imaging, *Chem. Mater.*, 2019, **31**, 4897.
19 B. d. Rosal, E. Ximendes, U. Rocha and D. Jaque, In Vivo Luminescence Nanothermometry: from Materials to Applications, *Adv. Opt. Mater.*, 2017, **5**, 1600508.
20 S. Xu, Y. Yu, Y. Gao, Y. Zhang, X. Li, J. Zhang, Y. Wang and B. Chen, Mesoporous silica coating $NaYF_4$:Yb,Er@$NaYF_4$ upconversion nanoparticles loaded with ruthenium(II) complex nanoparticles: Fluorometric sensing and cellular imaging of temperature by upconversion and of oxygen by downconversion, *Microchim. Acta*, 2018, **185**, 454.
21 P. Wang, H. Wang, Y. Fang, H. Li, J. He, Y. Ji, Y. Li, Q. Xu, J. Zheng and J. Lu, Thermoresponsive Memory Behavior in Metallosupramolecular Polymer-Based Ternary Memory Devices, *ACS Appl. Mater. Interfaces*, 2017, **9**, 32930.
22 Y. Ye, W. Zhang, Z. Zhao, J. Wang, C. Liu, Z. Deng, X. Zhao and J. Han, Highly Luminescent Cesium Lead Halide Perovskite Nanocrystals Stabilized in Glasses for Light-Emitting Applications, *Adv. Opt. Mater.*, 2019, **7**, 1801663.
23 A. Seeboth, R. Ruhmann and O. Mühling, Thermotropic and Thermochromic Polymer Based Materials for Adaptive Solar Control, *Materials*, 2010, **3**, 5143.
24 M. Li, Z. Yang, Y. Ren, J. Ruan, J. Qiu and Z. Song, Reversible Modulated Upconversion Luminescence of MoO_3:Yb^{3+},Er^{3+} Thermochromic Phosphor for Switching Devices, *Inorg. Chem.*, 2019, **58**, 6950.
25 J. Li, X. Liu, P. Cui, J. Li, T. Ye, X. Wang, C. Zhang and Y. S. Zhao, Lead-free thermochromic perovskites with tunable transition temperatures for smart window applications, *Sci. China: Chem.*, 2019, **62**, 1257.
26 S. T. Zimmermann, D. W. R. Balkenende, A. Lavrenova, C. Weder and J. Brugger, Nanopatterning of a Stimuli-Responsive Fluorescent Supramolecular Polymer by Thermal Scanning Probe Lithography, *ACS Appl. Mater. Interfaces*, 2017, **9**, 41454.
27 S. Srinivasan, P. A. Babu, S. Mahesh and A. Ajayaghosh, Reversible Self-Assembly of Entrapped Fluorescent Gelators in Polymerized Styrene Gel Matrix: Erasable Thermal Imaging via Recreation of Supramolecular Architectures, *J. Am. Chem. Soc.*, 2009, **131**, 15122.
28 B. Yoon, H. Shin, E.-M. Kang, D. W. Cho, K. Shin, H. Chung, C. W. Lee and J.-M. Kim, Inkjet-Compatible Single-Component Polydiacetylene Precursors for Thermochromic Paper Sensors, *ACS Appl. Mater. Interfaces*, 2013, **5**, 4527.
29 A. Seeboth, D. Lötzsch, R. Ruhmann and O. Muehling, Thermochromic Polymers—Function by Design, *Chem. Rev.*, 2014, **114**, 3037.

30 M. M. Ogle, A. D. S. McWilliams, B. Jiang and A. A. Martí, Latest Trends in Temperature Sensing by Molecular Probes, *ChemPhotoChem*, 2020, **4**, 255.
31 S. Liang, Y. Wang, X. Wu, M. Chen, L. Mu, G. She and W. Shi, An ultrasensitive ratiometric fluorescent thermometer based on frustrated static excimers in the physiological temperature range, *Chem. Commun.*, 2019, **55**, 3509.
32 A. Lavrenova, D. W. R. Balkenende, Y. Sagara, S. Schrettl, Y. C. Simon and C. Weder, Mechano- and Thermoresponsive Photoluminescent Supramolecular Polymer, *J. Am. Chem. Soc.*, 2017, **139**, 4302.
33 J.-F. Chen, X. Yin, B. Wang, K. Zhang, G. Meng, S. Zhang, Y. Shi, N. Wang, S. Wang and P. Chen, Planar Chiral Organoboranes with Thermoresponsive Emission and Circularly Polarized Luminescence: Integration of Pillar[5]arenes with Boron Chemistry, *Angew. Chem.*, 2020, **59**, 11267.
34 J. Zhang, A. Li, H. Zou, J. Peng, J. Guo, W. Wu, H. Zhang, J. Zhang, X. Gu, W. Xu, S. Xu, S. H. Liu, A. Qin, J. W. Y. Lama and B. Z. Tang, A "simple" donor–acceptor AIEgen with multi-stimuli responsive behaviour, *Mater. Horiz.*, 2020, **7**, 135.
35 J.-H. Kim, Y. Jung, D. Lee and W.-D. Jang, Thermoresponsive Polymer and Fluorescent Dye Hybrids for Tunable Multicolor Emission, *Adv. Mater.*, 2016, **28**, 3499.
36 S. Mukherjee and P. Thilagar, Stimuli and shape responsive 'boron-containing' luminescent organic materials, *J. Mater. Chem. C*, 2016, **4**, 2647.
37 T. Jiang, X. Wang, J. Wang, G. Hu and X. Ma, Humidity- and Temperature-Tunable Multicolor Luminescence of Cucurbit[8]uril-Based Supramolecular Assembly, *ACS Appl. Mater. Interfaces*, 2019, **11**, 14399.
38 Y. Li, Z. Li, Y. Hou, Y.-N. Fan and C.-Y. Su, Photoluminescent Phosphinine Cu(I) Halide Complexes: Temperature Dependence of the Photophysical Properties and Applications as a Molecular Thermometer, *Inorg. Chem.*, 2018, **57**, 13235.
39 Y. Ai, Y. Li, H. L.-K. Fu, A. K.-W. Chan and V. W.-W. Yam, Aggregation and Tunable Color Emission Behaviors of l -Glutamine-Derived Platinum(II) Bipyridine Complexes by Hydrogen-Bonding, π–π Stacking and Metal–Metal Interactions, *Chem. – Eur. J.*, 2019, **25**, 5251.
40 Z. Zhang, Z. Zhao, L. Wu, S. Lu, S. Ling, G. Li, L. Xu, L. Ma, Y. Hou, X. Wang, X. Li, G. He, K. Wang, B. Zou and M. Zhang, Emissive Platinum(II) Cages with Reverse Fluorescence Resonance Energy Transfer for Multiple Sensing, *J. Am. Chem. Soc.*, 2020, **142**, 2592.
41 M. Yamamoto, Y. Kitagawa, T. Nakanishi, K. Fushimi and Y. Hasegawa, Ligand-Assisted Back Energy Transfer in Luminescent TbIII Complexes for Thermosensing Properties, *Chem. – Eur. J.*, 2018, **24**, 17719.
42 K. Ohno, Y. Kusano, S. Kaizaki, A. Nagasawa and T. Fujihara, Chromism of Tartrate-Bridged Clamshell-like Platinum(II) Complex: Intramolecular Pt–Pt Interaction-Induced Luminescence Vapochromism and Intermolecular Interactions-Triggered Thermochromism, *Inorg. Chem.*, 2018, **57**, 14159.
43 K. Chen and V. J. Catalano, Luminescent Thermochromism in a Gold(I)–Copper(I) Phosphine–Pyridine Complex, *Eur. J. Inorg. Chem.*, 2015, 5254.
44 A. Kobayashi and M. Kato, Stimuli-responsive Luminescent Copper(I) Complexes for Intelligent Emissive Devices, *Chem. Lett.*, 2017, **46**, 154.
45 W. P. Lustig, S. Mukherjee, N. D. Rudd, A. V. Desai, J. Li and S. K. Ghosh, Metal–organic frameworks: functional luminescent and photonic materials for sensing applications, *Chem. Soc. Rev.*, 2017, **46**, 3242.
46 J. Rocha, C. D. S. Brites and L. D. Carlos, Lanthanide Organic Framework Luminescent Thermometers, *Chem. – Eur. J.*, 2016, **22**, 14782.
47 L. Qiu, C. Yu, X. Wang, Y. Xie, A. M. Kirillov, W. Huang, J. Li, P. Gao, T. Wu, X. Gu, Q. Nie and D. Wu, Tuning the Solid-State White Light Emission of Postsynthetic Lanthanide-Encapsulated Double-Layer MOFs for Three-Color Luminescent Thermometry Applications, *Inorg. Chem.*, 2019, **58**, 4524.
48 C. Li, K. Wang, J. Li and Q. Zhang, Recent Progress in Stimulus-Responsive Two-Dimensional Metal–Organic Frameworks, *ACS Mater. Lett.*, 2020, **2**, 779.
49 M.-E. Sun, Y. Li, X.-Y. Dong and S.-Q. Zang, Thermoinduced structural-transformation and thermochromic luminescence in organic manganese chloride crystals, *Chem. Sci.*, 2019, **10**, 3836.
50 G. Wang, Z. Li, X. Luo, R. Yue, Y. Shen and N. Ma, DNA-templated nanoparticle complexes for photothermal imaging and labeling of cancer cells, *Nanoscale*, 2018, **10**, 16508.
51 Y. S. Borghei and M. Hosseini, An approach toward miRNA detection via different thermo-responsive aggregation/disaggregation of CdTe quantum dots, *RSC Adv.*, 2018, **8**, 30148.
52 C. Bradac, S. F. Lim, H.-C. Chang and I. Aharonovich, Optical Nanoscale Thermometry: From Fundamental Mechanisms to Emerging Practical Applications, *Adv. Opt. Mater.*, 2020, **8**, 202000183.
53 C. Wang, L. Ling, Y. Yao and Q. Song, One-step synthesis of fluorescent smart thermo-responsive copper clusters: A potential nanothermometer in living cells, *Nano Res.*, 2015, **8**, 1975.
54 J. Ye, X. Dong, H. Jiang and X. Wang, An intracellular temperature nanoprobe based on biosynthesized fluorescent copper nanoclusters, *J. Mater. Chem. B*, 2017, **5**, 691.
55 E. Hemmer, M. Quintanilla, F. Légaré and F. Vetrone, Temperature-Induced Energy Transfer in Dye-Conjugated Upconverting Nanoparticles: A New Candidate for Nanothermometry, *Chem. Mater.*, 2015, **27**, 235.
56 V. W.-W. Yam, V. K.-M. Au and S. Y.-L. Leung, Light-Emitting Self-Assembled Materials Based on d^8 and d^{10} Transition Metal Complexes, *Chem. Rev.*, 2015, **115**, 7589.

57 Y. Han, Z. Gao, C. Wang, R. Zhong and F. Wang, Recent progress on supramolecular assembly of organoplatinum (II) complexes into long-range ordered nanostructures, *Coord. Chem. Rev.*, 2020, **414**, 213300.
58 O. S. Wenger, Photoactive Complexes with Earth-Abundant Metals, *J. Am. Chem. Soc.*, 2018, **140**, 13522.
59 K. Y. Zhang, S. Liu, Q. Zhao and W. Huang, Stimuli–responsive metallopolymers, *Coord. Chem. Rev.*, 2016, **319**, 180.
60 C. D. S. Brites, S. Balabhadra and L. D. Carlos, Lanthanide-Based Thermometers: At the Cutting-Edge of Luminescence Thermometry, *Adv. Opt. Mater.*, 2019, **7**, 1801239.
61 C. Yuan, S. Saito, C. Camacho, S. Irle, I. Hisaki and S. Yamaguchi, A π-Conjugated System with Flexibility and Rigidity That Shows Environment-Dependent RGB Luminescence, *J. Am. Chem. Soc.*, 2013, **135**, 8842.
62 Y. Cao, J. K. Nagle, M. O. Wolf and B. O. Patrick, Tunable Luminescence of Bithiophene-Based Flexible Lewis Pairs, *J. Am. Chem. Soc.*, 2015, **137**, 4888.
63 A. K.-W. Chan, D. Wu, K. M.-C. Wong and V. W.-W. Yam, Rhodium(I) Complexes of Tridentate N-Donor Ligands and Their Supramolecular Assembly Studies, *Inorg. Chem.*, 2016, **55**, 3685.
64 L. Liu, X. Wang, F. Hussain, C. Zeng, B. Wang, Z. Li, I. Kozin and S. Wang, Multiresponsive Tetradentate Phosphorescent Metal Complexes as Highly Sensitive and Robust Luminescent Oxygen Sensors: Pd(II) Versus Pt(II) and 1,2,3-Triazolyl Versus 1,2,4-Triazolyl, *ACS Appl. Mater. Interfaces*, 2019, **11**, 12666.
65 B. Xin, J. Sang, Y. Gao, G. Li, Z. Shi and S. Feng, A pillared-layered copper(I) halide-based metal–organic framework exhibiting dual emission, and piezochromic and thermochromic properties with a large temperature-dependent emission red-shift, *RSC Adv.*, 2018, **8**, 1973.
66 Q. Ma, M. Zhang, X. Xu, K. Meng, C. Yao, Y. Zhao, J. Sun, Y. Du and D. Yang, Multiresponsive Supramolecular Luminescent Hydrogels Based on a Nucleoside/Lanthanide Complex, *ACS Appl. Mater. Interfaces*, 2019, **11**, 47404.
67 P. Chen, Q. Li, S. Grindy and N. Holten-Andersen, White-Light-Emitting Lanthanide Metallogels with Tunable Luminescence and Reversible Stimuli-Responsive Properties, *J. Am. Chem. Soc.*, 2015, **137**, 11590.
68 G. A. Filonenko, D. Sun, M. Weber, C. Müller and E. A. Pidko, Multicolor Organometallic Mechanophores for Polymer Imaging Driven by Exciplex Level Interactions, *J. Am. Chem. Soc.*, 2019, **141**, 9687.
69 J. Pitchaimani, S. Karthikeyan, N. Lakshminarasimhan, S. P. Anthony, D. Moon and V. Madhu, Reversible Thermochromism of Nickel(II) Complexes and Single-Crystal-to-Single-Crystal Transformation, *ACS Omega*, 2019, **4**, 13756.
70 A. Y.-Y. Tam, K. M.-C. Wong and V. W.-W. Yam, Unusual Luminescence Enhancement of Metallogels of Alkynylplatinum(II) 2,6-Bis(N-alkylbenzimidazol-2′-yl)pyridine Complexes upon a Gel-to-Sol Phase Transition at Elevated Temperatures, *J. Am. Chem. Soc.*, 2009, **131**, 6253.
71 M.-S. Jiang, Y.-H. Tao, Y.-W. Wang, C. Lu, D. J. Young, J.-P. Lang and Z.-G. Ren, Reversible Solid-State Phase Transitions between Au–P Complexes Accompanied by Switchable Fluorescence, *Inorg. Chem.*, 2020, **59**, 3072.
72 Y. Pan, H.-Q. Su, E.-L. Zhou, H.-Z. Yin, K.-Z. Shao and Z.-M. Su, A stable mixed lanthanide metal–organic framework for highly sensitive thermometry, *Dalton Trans.*, 2019, **48**, 3723.
73 Y. Cui, H. Xu, Y. Yue, Z. Guo, J. Yu, Z. Chen, J. Gao, Y. Yang, G. Qian and B. Chen, A Luminescent Mixed-Lanthanide Metal–Organic Framework Thermometer, *J. Am. Chem. Soc.*, 2012, **134**, 3979.
74 K. Yang, S.-L. Li, F.-Q. Zhang and X.-M. Zhang, Simultaneous Luminescent Thermochromism, Vapochromism, Solvatochromism, and Mechanochromism in a C_3-Symmetric Cubane $[Cu_4I_4P_4]$ Cluster without Cu–Cu Interaction, *Inorg. Chem.*, 2016, **55**, 7323.
75 Q. Benito, A. Fargues, A. Garcia, S. Maron, T. Gacoin, J.-P. Boilot, S. Perruchas and F. Camerel, Photoactive Hybrid Gelators Based on a Luminescent Inorganic $[Cu_4I_4]$ Cluster Core, *Chem. – Eur. J.*, 2013, **19**, 15831.
76 G.-G. Luo, H.-F. Su, A. Xiao, Z. Wang, Y. Zhao, Q.-Y. Wu, J.-H. Wu, D. Sun and L.-S. Zheng, Silver–Sulfur Hybrid Supertetrahedral Clusters: The Hitherto Missing Members in the Metal–Chalcogenide Tetrahedral Clusters, *Chem. – Eur. J.*, 2017, **23**, 14420.
77 A. V. Artem'ev, M. R. Ryzhikov, A. S. Berezin, I. E. Kolesnikov, D. G. Samsonenko and I. Y. Bagryanska, Photoluminescence of Ag(I) complexes with a square-planar coordination geometry: the first observation, *Inorg. Chem. Front.*, 2019, **6**, 2855.
78 K. Okabe, N. Inada, C. Gota, Y. Harada, T. Funatsu and S. Uchiyama, Intracellular temperature mapping with a fluorescent polymeric thermometer and fluorescence lifetime imaging microscopy, *Nat. Commun.*, 2012, **3**, 705.
79 H. Zhang, J. Jiang, P. Gao, T. Yang, K. Y. Zhang, Z. Chen, S. Liu, W. Huang and Q. Zhao, Dual-Emissive Phosphorescent Polymer Probe for Accurate Temperature Sensing in Living Cells and Zebrafish Using Ratiometric and Phosphorescence Lifetime Imaging Microscopy, *ACS Appl. Mater. Interfaces*, 2018, **10**, 17542.
80 J. S. Donner, S. A. Thompson, M. P. Kreuzer, G. Baffou and R. Quidant, Mapping Intracellular Temperature Using Green Fluorescent Protein, *Nano Lett.*, 2012, **12**, 2107.
81 C. Fan and C. Yang, Yellow/orange emissive heavy-metal complexes as phosphors in monochromatic and white organic light-emitting devices, *Chem. Soc. Rev.*, 2014, **43**, 6439.
82 C.-W. Lu, Y. Wang and Y. Chi, Metal Complexes with Azolate-Functionalized Multidentate Ligands: Tactical Designs and Optoelectronic Applications, *Chem. – Eur. J.*, 2016, **22**, 17892.
83 S. Guo, M. Han, R. Chen, Y. Zhuang, L. Zou, S. Liu, W. Huang and Q. Zhao, Mitochondria-localized iridium

(III) complexes with anthraquinone groups as effective photosensitizers for photodynamic therapy under hypoxia, *Sci. China: Chem.*, 2019, **62**, 1639.

84 F. Wei, S.-L. Lai, S. Zhao, M. Ng, M.-Y. Chan, V. W.-W. Yam and K. M.-C. Wong, Ligand Mediated Luminescence Enhancement in Cyclometalated Rhodium (III) Complexes and Their Applications in Efficient Organic Light-Emitting Devices, *J. Am. Chem. Soc.*, 2019, **141**, 12863.

85 N. Bustamante, G. Ielasi, M. Bedoya and G. Orellana, Optimization of Temperature Sensing with Polymer-Embedded Luminescent Ru(II) Complexes, *Polymers*, 2018, **10**, 234.

86 M. Mirenda, V. Levi, M. L. Bossi, L. Bruno, A. V. Bordoni, A. E. Regazzoni and A. Wolosiuk, Temperature response of luminescent tris(bipyridine)ruthenium(II)-doped silica nanoparticles, *J. Colloid Interface Sci.*, 2013, **392**, 96.

87 F. Sguerra, R. Marion, G. H. V. Bertrand, R. Coulon, É. Sauvageot and R. Daniellou, Thermo- and radioluminescent polystyrene based plastic scintillators doped with phosphorescent iridium(III) complexes, *J. Mater. Chem. C*, 2014, **2**, 6125.

88 L. H. Fischer, M. I. J. Stich, O. S. Wolfbeis, N. Tian, E. Holder and M. Schäferling, Red- and Green-Emitting Iridium(III) Complexes for a Dual Barometric and Temperature-Sensitive Paint, *Chem. – Eur. J.*, 2009, **15**, 10857.

89 K. Y. Zhang, X. Chen, G. Sun, T. Zhang, S. Liu, Q. Zhao and W. Huang, Utilization of Electrochromically Luminescent Transition-Metal Complexes for Erasable Information Recording and Temperature-Related Information Protection, *Adv. Mater.*, 2016, **28**, 7137.

90 J. E. Yarnell, C. E. McCusker, A. J. Leeds, J. M. Breaux and F. N. Castellano, Exposing the Excited-State Equilibrium in an IrIII Bichromophore: A Combined Time Resolved Spectroscopy and Computational Study, *Eur. J. Inorg. Chem.*, 2016, 1808.

91 L. Liu, X. Wang, N. Wang, T. Peng and S. Wang, Bright, Multi-responsive, Sky-Blue Platinum(II) Phosphors Based on a Tetradentate Chelating Framework, *Angew. Chem., Int. Ed.*, 2017, **56**, 9160.

92 S. C. Cuerva, J. A. Campo, M. Cano, M. Caño-García, J. M. Otón and C. Lodeiro, Aggregation-induced emission enhancement (AIEE)-active Pt(II) metallomesogens as dyes sensitive to Hg^{2+} and dopant agents to develop stimuli-responsive luminescent polymer materials, *Dyes Pigm.*, 2020, **175**, 108098.

93 M. H.-Y. Chan, S. Y.-L. Leung and V. W.-W. Yam, Rational Design of Multi-Stimuli-Responsive Scaffolds: Synthesis of Luminescent Oligo(ethynylpyridine)-Containing Alkynylplatinum(II) Polypyridine Foldamers Stabilized by Pt···Pt Interactions, *J. Am. Chem. Soc.*, 2019, **141**, 12312.

94 Z. Chen, J.-H. Tang, W. Chen, Y. Xu, H. Wang, Z. Zhang, H. Sepehrpour, G.-J. Cheng, X. Li, P. Wang, Y. Sun and P. J. Stang, Temperature- and Mechanical-Force-Responsive Self-Assembled Rhomboidal Metallacycle, *Organometallics*, 2019, **38**, 4244.

95 K.-C. Chang, J.-L. Lin, Y.-T. Shen, C.-Y. Hung, C.-Y. Chen and S.-S. Sun, Synthesis and Photophysical Properties of Self-Assembled Metallogels of Platinum(II) Acetylide Complexes with Elaborate Long-Chain Pyridine-2,6-Dicarboxamides, *Chem. – Eur. J.*, 2012, **18**, 1312.

96 F. Zhong, J. Zhao, M. Hayvali, A. Elmali and A. Karatay, Effect of Molecular Conformation Restriction on the Photophysical Properties of N^N Platinum(II) Bis(ethynyl-naphthalimide) Complexes Showing Close-Lying ^{3}MLCT and ^{3}LE Excited States, *Inorg. Chem.*, 2019, **58**, 1850.

97 J.-H. Tang, Y. Sun, Z.-L. Gong, Z.-Y. Li, Z. Zhou, H. Wang, X. Li, M. L. Saha, Y.-W. Zhong and P. J. Stang, Temperature-Responsive Fluorescent Organoplatinum(II) Metallacycles, *J. Am. Chem. Soc.*, 2018, **140**, 7723.

98 S. Lin, H. Pan, L. Li, R. Liao, S. Yu, Q. Zhao, H. Sun and W. Huang, AIPE-active platinum(II) complexes with tunable photophysical properties and their application in constructing thermosensitive probes used for intracellular temperature imaging, *J. Mater. Chem. C*, 2019, **7**, 7893.

99 C. M. Brown, V. Carta and M. O. Wolf, Thermochromic Solid-State Emission of Dipyridyl Sulfoxide Cu(I) Complexes, *Chem. Mater.*, 2018, **30**, 5786.

100 I. D. Strelnik, V. V. Sizov, V. V. Gurzhiy, A. S. Melnikov, I. E. Kolesnikov, E. I. Musina, A. A. Karasik and E. V. Grachova, Binuclear Gold(I) Phosphine Alkynyl Complexes Templated on a Flexible Cyclic Phosphine Ligand: Synthesis and Some Features of Solid-State Luminescence, *Inorg. Chem.*, 2020, **59**, 244.

101 J. Cored, O. Crespo, J. L. Serrano, A. Elduque and Ra. Giménez, Decisive Influence of the Metal in Multifunctional Gold, Silver, and Copper Metallacycles: High Quantum Yield Phosphorescence, Color Switching, and Liquid Crystalline Behavior, *Inorg. Chem.*, 2018, **57**, 12632.

102 Y. Ma, Y. Dong, S. Liu, P. She, J. Lu, S. Liu, W. Huang and Q. Zhao, Chameleon-Like Thermochromic Luminescent Materials with Controllable Response Behaviors for Multilevel Security Printing, *Adv. Opt. Mater.*, 2020, **8**, 1901687.

103 J. Miao, Y. Nie, Y. Li, C. Qin, Y. Ren, C. Xu, M. Yan, K. Liu and G. Liu, Single-component solid state white-light emission and photoluminescence color tuning of a Cd(II) complex and its application as a luminescence thermometer, *J. Mater. Chem. C*, 2019, **7**, 13454.

104 S. Otto, N. Scholz, T. Behnke, U. Resch-Genger and K. Heinze, Thermo-Chromium: A Contactless Optical Molecular Thermometer, *Chem. – Eur. J.*, 2017, **23**, 12131.

105 (*a*) A. S. Berezin, D. G. Samsonenko, V. K. Brel and A. V. Artem'ev, "Two-in-one" organic–inorganic hybrid Mn^{II} complexes exhibiting dual-emissive phosphorescence, *Dalton Trans.*, 2018, **47**, 7306; (*b*) Y. Wu, X. Zhang, Y.-Q. Zhang, M. Yang and Z.-N. Chen, Achievement of ligand-field induced thermochromic luminescence via two-step single-crystal to single-crystal transformations, *Chem. Commun.*, 2018, **54**, 13961.

106 S. Katagiri, Y. Hasegawa, Y. Wada and S. Yanagida, Thermo-sensitive Luminescence Based on the Back

Energy Transfer in Terbium(III) Complexes, *Chem. Lett.*, 2004, **33**, 1438.

107 D. V. Lapaev, V. G. Nikiforov, V. S. Lobkov, A. A. Knyazev and Y. G. Galyametdinov, A photostable vitrified film based on a terbium(III) β-diketonate complex as a sensing element for reusable luminescent thermometers, *J. Mater. Chem. C*, 2018, **6**, 9475.

108 M. Tang, Y. Huang, Y. Wang and L. Fu, An ytterbium complex with unique luminescence properties: detecting the temperature based on a luminescence spectrum without the interference of oxygen, *Dalton Trans.*, 2015, **44**, 7449.

109 Y. Kitagawa, M. Kumagai, T. Nakanishi, K. Fushimi and Y. Hasegawa, The Role of π–f Orbital Interactions in Eu (III) Complexes for an Effective Molecular Luminescent Thermometer, *Inorg. Chem.*, 2020, **59**, 5865.

110 D. V. Lapaev, V. G. Nikiforov, V. S. Lobkov, A. A. Knyazev, R. M. Ziyatdinova and Y. G. Galyametdinov, A vitrified film of an anisometric europium(III) β-diketonate complex with a low melting point as a reusable luminescent temperature probe with excellent sensitivity in the range of 270–370 K, *J. Mater. Chem. C*, 2020, **8**, 6273.

111 J. R. Shakirova, N. N. Shevchenko, V. A. Baigildin, P. S. Chelushkin, A. F. Khlebnikov, O. A. Tomashenko, A. I. Solomatina, G. L. Starova and S. P. Tunik, Eu-Based Phosphorescence Lifetime Polymer Nanothermometer: A Nanoemulsion Polymerization Approach to Eliminate Quenching of Eu Emission in Aqueous Media, *ACS Appl. Polym. Mater.*, 2020, **2**(2), 537.

112 S. Swavey, J. A. Krause, D. Collins, D. D'Cunha and A. Fratini, X-ray structure and temperature dependent luminescent properties of two bimetallic europium complexes, *Polyhedron*, 2008, **27**, 1061.

113 K. Yanagisawa, Y. Kitagawa, T. Nakanishi, T. Seki, K. Fushimi, H. Ito and Y. Hasegawa, A Luminescent Dinuclear EuIII/TbIII Complex with LMCT Band as a Single-Molecular Thermosensor, *Chem. – Eur. J.*, 2018, **24**, 1956.

114 R. Peng, M. Li and D. Li, Copper(I) halides: A versatile family in coordination chemistry and crystal engineering, *Coord. Chem. Rev.*, 2010, **254**, 1.

115 M. Wallesch, D. Volz, D. M. Zink, U. Schepers, M. Nieger, T. Baumann and S. Brase, Bright Coppertunities: Multinuclear CuI Complexes with N–P Ligands and Their Applications, *Chem. – Eur. J.*, 2014, **20**, 6578.

116 B. Huitorel, Q. Benito, A. Fargues, A. Garcia, T. Gacoin, J.-P. Boilot, S. Perruchas and F. Camerel, Mechanochromic Luminescence and Liquid Crystallinity of Molecular Copper Clusters, *Chem. Mater.*, 2016, **28**, 8190.

117 A. V. Shamsieva, I. E. Kolesnikov, I. D. Strelnik, T. P. Gerasimova, A. A. Kalinichev, S. A. Katsyuba, E. I. Musina, E. Lähderanta, A. A. Karasik and O. G. Sinyashin, Fresh Look on the Nature of Dual-Band Emission of Octahedral Copper-Iodide Clusters—Promising Ratiometric Luminescent Thermometers, *J. Phys. Chem. C*, 2019, **123**, 25863.

118 S.-Z. Zhan, X. Jiang, J. Zheng, X.-D. Huang, G.-H. Chen and D. Li, A luminescent supramolecular $Cu_2I_2(NH_3)_2$-sandwiched Cu_3(pyrazolate)$_3$ adduct as a temperature sensor, *Dalton Trans.*, 2018, **47**, 3679.

119 C.-Y. Yue, F.-L. Liu, W.-T. Deng, J. Tao and M.-C. Hong, Iodide-Centered Cuprous Octatomic Ring: A Luminescent Molecular Thermometer Exhibiting Dual-Emission Character, *Cryst. Growth Des.*, 2018, **18**, 22.

120 L. Shang, F. Stockmar, N. Azadfar and G. U. Nienhaus, Intracellular Thermometry by Using Fluorescent Gold Nanoclusters, *Angew. Chem., Int. Ed.*, 2013, **52**, 11154.

121 Y.-T. Wu, C. Shanmugam, W.-B. Tseng, M.-M. Hiseh and W.-L. Tseng, A gold nanocluster-based fluorescent probe for simultaneous pH and temperature sensing and its application to cellular imaging and logic gates, *Nanoscale*, 2016, **8**, 11210.

122 S. Kundu, D. Mukherjee, T. K. Maiti and N. Sarkar, Highly Luminescent Thermoresponsive Green Emitting Gold Nanoclusters for Intracellular Nanothermometry and Cellular Imaging: A Dual Function Optical Probe, *ACS Appl. Bio Mater.*, 2019, **2**, 2078.

123 D.-F. Lu, Z.-F. Hong, J. Xie, X.-J. Kong, L.-S. Long and L.-S. Zheng, High-Nuclearity Lanthanide–Titanium Oxo Clusters as Luminescent Molecular Thermometers with High Quantum Yields, *Inorg. Chem.*, 2017, **56**, 12186.

124 S. M. Bruno, D. Ananias, F. A. A. Paz, M. Pillinger, A. A. Valente, L. D. Carlos and I. S. Gonçalves, Crystal structure and temperature-dependent luminescence of a heterotetranuclear sodium–europium(III) β-diketonate complex, *Dalton Trans.*, 2015, **44**, 488.

125 W. Huang, M. Zhang, S. Huang and D. Wu, Tunable Luminescent Heterometallic Zn_2Ln_2 Edge-Defective Molecular Cubane with Stimuli-Responsive Properties, *Inorg. Chem.*, 2017, **56**, 6768.

126 H. Yao, G. Calvez, C. Daiguebonne, K. Bernot, Y. Suffren and O. Guillou, Hetero-hexalanthanide Complexes: A New Synthetic Strategy for Molecular Thermometric Probes, *Inorg. Chem.*, 2019, **58**, 16180.

127 J. Conesa-Egea, N. Nogal, J. I. Martínez, V. Fernández-Moreira, U. R. Rodríguez-Mendoza, J. González-Platas, C. J. Gómez-García, S. Delgado, F. Zamora and P. Amo-Ochoa, Smart composite films of nanometric thickness based on copper–iodine coordination polymers. Toward sensors, *Chem. Sci.*, 2018, **9**, 8000.

128 S.-S. Zhao, L. Wang, Y. Liu, L. Chen and Z. Xie, Stereochemically Dependent Synthesis of Two Cu(I) Cluster-Based Coordination Polymers with Thermochromic Luminescence, *Inorg. Chem.*, 2017, **56**, 13975.

129 O. Veselska, D. Podbevšek, G. Ledoux, A. Fateeva and A. Demessence, Intrinsic triple-emitting 2D copper thiolate coordination polymer as a ratiometric thermometer working over 400 K range, *Chem. Commun.*, 2017, **53**, 12225.

130 Z.-H. Yan, X.-Y. Li, L.-W. Liu, S.-Q. Yu, X.-P. Wang and D. Sun, Single-Crystal to Single-Crystal Phase Transition and Segmented Thermochromic Luminescence in a

Dynamic 3D Interpenetrated AgI Coordination Network, *Inorg. Chem.*, 2016, **55**, 1096.

131 X.-Y. Dong, H.-L. Huang, J.-Y. Wang, H.-Y. Li and S.-Q. Zang, A Flexible Fluorescent SCC-MOF for Switchable Molecule Identification and Temperature Display, *Chem. Mater.*, 2018, **30**, 2160.

132 Y. Wang, B. Wang, H. Shi, C. Zhang, C. Tao and J. Li, Carbon nanodots in ZIF-8: synthesis, tunable luminescence and temperature sensing, *Inorg. Chem. Front.*, 2018, **5**, 2739.

133 L. Tom and M. R. P. Kurup, A reversible thermo-responsive 2D Zn(II) coordination polymer as a potential self-referenced luminescent thermometer, *J. Mater. Chem. C*, 2020, **8**, 2525.

134 H. Zhang, C. Lin, T. Sheng, S. Hu, C. Zhuo, R. Fu, Y. Wen, H. Li, S. Su and X. Wu, A Luminescent Metal–Organic Framework Thermometer with Intrinsic Dual Emission from Organic Lumophores, *Chem. – Eur. J.*, 2016, **22**, 4460.

135 L. Chen, J.-W. Ye, H.-P. Wang, M. Pan, S.-Y. Yin, Z.-W. Wei, L.-Y. Zhang, K. Wu, Y.-N. Fan and C.-Y. Su, Ultrafast water sensing and thermal imaging by a metal-organic framework with switchable luminescence, *Nat. Commun.*, 2017, **8**, 15985.

136 D. Li, X. Yang and D. Yan, Cluster-Based Metal–Organic Frameworks: Modulated Singlet–Triplet Excited States and Temperature-Responsive Phosphorescent Switch, *ACS Appl. Mater. Interfaces*, 2018, **10**, 34377.

137 H. Cai, W. Lu, C. Yang, M. Zhang, M. Li, C.-M. Che and D. Li, Tandem Förster Resonance Energy Transfer Induced Luminescent Ratiometric Thermometry in Dye-Encapsulated Biological Metal–Organic Frameworks, *Adv. Opt. Mater.*, 2019, **7**, 1801149.

138 H. Zhang, L. Zhou, J. Wei, Z. Li, P. Lin and S. Du, Highly luminescent and thermostable lanthanide-carboxylate framework materials with helical configurations, *J. Mater. Chem.*, 2012, **22**, 21210.

139 A. Balamurugan, M. L. P. Reddy and M. Jayakannan, π-Conjugated polymer–Eu^{3+} complexes: versatile luminescent molecular probes for temperature sensing, *J. Mater. Chem. A*, 2013, **1**, 2256.

140 T. Xia, Y. Cui, Y. Yang and G. Qian, A luminescent ratiometric thermometer based on thermally coupled levels of a Dy-MOF, *J. Mater. Chem. C*, 2017, **5**, 5044.

141 L. Li, Y. Zhu, X. Zhou, C. D. S. Brites, D. Ananias, Z. Lin, F. A. A. Paz, J. Rocha, W. Huang and L. D. Carlos, Visible-Light Excited Luminescent Thermometer Based on Single Lanthanide Organic Frameworks, *Adv. Funct. Mater.*, 2016, **26**, 8677.

142 D. Ananias, A. D. G. Firmino, R. F. Mendes, F. A. A. Paz, M. Nolasco, L. D. Carlos and J. Rocha, Excimer Formation in a Terbium Metal–Organic Framework Assists Luminescence Thermometry, *Chem. Mater.*, 2017, **29**, 9547.

143 K. Miyata, Y. Konno, T. Nakanishi, A. Kobayashi, M. Kato, K. Fushimi and Y. Hasegawa, Chameleon Luminophore for Sensing Temperatures: Control of Metal-to-Metal and Energy Back Transfer in Lanthanide Coordination Polymers, *Angew. Chem., Int. Ed.*, 2013, **52**, 6413.

144 F. V. Bussche, A. M. Kaczmarek, J. Schmidt, C. V. Stevens and P. Van Der Voort, Lanthanide grafted phenanthroline-polymer for physiological temperature range sensing, *J. Mater. Chem. C*, 2019, **7**, 10972.

145 J. K. Zaręba, M. Nyk, J. Janczak and M. Samoć, Three-Photon Absorption of Coordination Polymer Transforms UV-to-VIS Thermometry into NIR-to-VIS Thermometry, *ACS Appl. Mater. Interfaces*, 2019, **11**, 10435.

146 D. Zhao, D. Yue, L. Zhang, K. Jiang and G. Qian, Cryogenic Luminescent Tb/Eu-MOF Thermometer Based on a Fluorine-Modified Tetracarboxylate Ligand, *Inorg. Chem.*, 2018, **57**, 12596.

147 X.-D. Wang, R. J. Meier, M. Schäferling, S. Bange, J. M. Lupton, M. Sperber, J. Wegener, V. Ondrus, U. Beifuss, U. Henne, C. Klein and O. S. Wolfbeis, Two-Photon Excitation Temperature Nanosensors Based on a Conjugated Fluorescent Polymer Doped with a Europium Probe, *Adv. Opt. Mater.*, 2016, **4**, 1854.

148 S. Li, X.-F. Jiang and Q.-H. Xu, Polyfluorene based conjugated polymer nanoparticles for two-photon live cell imaging, *Sci. China: Chem.*, 2018, **61**, 88.

149 M.-J. Sun, Y.-W. Zhong and J. Yao, Thermal-Responsive Phosphorescent Nanoamplifiers Assembled from Two Metallophosphors, *Angew. Chem., Int. Ed.*, 2018, **57**, 7820.

150 Z. Li, Z. Hou, D. Ha and H. Li, A Ratiometric Luminescent Thermometer Co-doped with Lanthanide and Transition Metals, *Chem. – Asian J.*, 2015, **10**, 2720.

151 Z. Chen, K. Y. Zhang, X. Tong, Y. Liu, C. Hu, S. Liu, Q. Yu, Q. Zhao and W. Huang, Phosphorescent Polymeric Thermometers for In Vitro and In Vivo Temperature Sensing with Minimized Background Interference, *Adv. Funct. Mater.*, 2016, **26**, 4386.

152 (*a*) H. Yersin, R. Czerwieniec, M. Z. Shafikov and A. F. Suleymanova, TADF Material Design: Photophysical Background and Case Studies Focusing on Cu^{I} and Ag^{I} complexes, *ChemPhysChem*, 2017, **18**, 3508; (*b*) G. Li, Z.-Q. Zhu, Q. Chen and J. Li, Metal complex based on delayed fluorescence materials, *Org. Electron.*, 2019, **69**, 135.